Chem. Senses 36: 43–61, 2011

doi:10.1093/chemse/bjq096
Advance Access publication October 20, 2010

Organization of Deutocerebral Neuropils and Olfactory Behavior in the Centipede *Scutigera coleoptrata* (Linnaeus, 1758) (Myriapoda: Chilopoda)

Andy Sombke[1,2], Steffen Harzsch[2] and Bill S. Hansson[1]

[1]Department of Evolutionary Neuroethology, Max Planck Institute for Chemical Ecology, Hans-Knöll-Straße 8, 07745 Jena, Germany and [2]Zoologisches Institut und Museum, Cytologie und Evolutionsbiologie, Ernst Moritz Arndt Universität Greifswald, Johann-Sebastian-Bach-Straße 11/12, 17497 Greifswald, Germany

Correspondence to be sent to: Andy Sombke, Department of Evolutionary Neuroethology, Max Planck Institute for Chemical Ecology, Hans-Knöll-Straße 8, 07745 Jena, Germany. e-mail: andy.sombke@uni-greifswald.de

Accepted August 22, 2010

Abstract

Myriapods represent an arthropod lineage, that originating from a marine arthropod ancestor most likely conquered land independently from hexapods and crustaceans. Establishing aerial olfaction during a transition from the ocean to land requires molecules to be detected in gas phase instead of in water solution. Considering that the olfactory sense of myriapods has evolved independently from that in hexapods and crustaceans, the question arises if and how myriapods have solved the tasks of odor detection and odor information processing in air. Comparative studies between arthropod taxa that independently have established a terrestrial life style provide a powerful means of investigating the evolution of chemosensory adaptations in this environment and to understand how the arthropod nervous system evolved in response to new environmental and ecological challenges. In general, the neuroethology of myriapods and the architecture of their central nervous systems are insufficiently understood. In a set of experiments with the centipede *Scutigera coleoptrata*, we analyzed the central olfactory pathway with serial semi-thin sectioning combined with 3-dimensional reconstruction, antennal backfilling with neuronal tracers, and immunofluorescence combined with confocal laser-scanning microscopy. Furthermore, we conducted behavioral experiments to find out if these animals react to airborne stimuli. Our results show that the primary olfactory and mechanosensory centers are well developed in these organisms but that the shape of the olfactory neuropils in *S. coleoptrata* is strikingly different when compared with those of hexapods and malacostracan crustaceans. Nevertheless, the presence of distinct neuropils for chemosensory and mechanosensory qualities in *S. coleoptrata*, malacostracan Crustacea, and Hexapoda could indicate a common architectural principle within the Mandibulata. Furthermore, behavioral experiments indicate that *S. coleoptrata* is able to perceive airborne stimuli, both from live prey and from a chemical extract of the prey. These results are in line with the morphological findings concerning the well-developed olfactory centers in the deutocerebrum of this species.

Key words: behavior, Chilopoda, deutocerebrum, nervous system, neurophylogeny, olfaction

Introduction

In many arthropods, primary olfactory centers are characterized by their subdivision into structural and functional subunits (Schachtner et al. 2005). In Hexapoda, the subunits of the neuropil that is targeted by the axons of olfactory sensory neurons (OSNs), the antennal lobe, are called glomeruli (reviewed in Homberg 1994; Anton and Homberg 1999; Vosshall and Stocker 2007). In malacostracan crustaceans, these subunits in the olfactory lobe are also called glomeruli or sometimes "olfactory columns" (Sandeman et al. 1992, 1993; Schmidt and Ache 1996b; Harzsch and Hansson 2008). Within the glomeruli of both Hexapoda and malacostracan Crustacea, first-order integration of olfactory input takes place, which is then relayed to secondary brain centers. Within the primary centers, the afferents of OSNs target dendritic arborizations of local interneurons and projection neurons (Schachtner et al. 2005) representing the first step in the complex mechanisms of odor recognition and discrimination (Hansson and Christensen 1999; Ignell and Hansson 2005). The glomerular array in Hexapoda is thought to represent a chemotopic map, which forms the basis of the olfactory code (Galizia and Menzel 2000, 2001; Ignell and Hansson 2005). Due to the common architecture of primary olfactory

brain centers (antennal lobe in Hexapoda, olfactory lobe in Crustacea) in corresponding sets of olfactory interneurons, the glomeruli may represent homologous structures of Hexapoda and malacostracan Crustacea (Schachtner et al. 2005; Strausfeld 2009). However, differences in their neuronal organization may also suggest independent origins and thus convergent evolution (Strausfeld 2009). Similarities can also be found when comparing vertebrate and arthropod olfactory neuropils (ONs). These conformities in architecture across widely separated phyla could be the result of common selective pressures to perform the same tasks (Strausfeld and Hildebrand 1999; Eisthen 2002). The deutocerebrum also processes mechanosensory input. In Hexapoda, the antennal mechanosensory and motor center (AMMC) integrates information from antennal mechanoreceptors and other areas of the head capsule (Homberg 2005). In Crustacea, the lateral and median antennular neuropils (LAN and MAN) receive mechanosensory and nonolfactory chemosensory input from the antennules (antenna 1; e.g., Schmidt et al. 1992; Schmidt and Ache 1996a).

Many recent phylogenetic studies have suggested a sister group relationship between Crustacea and Hexapoda, the 2 taxa together being called Tetraconata (reviews Dohle 2001; Richter 2002). The position of Myriapoda in the system of arthropods is still in debate (reviewed in Edgecombe and Giribet 2007). Traditionally, Myriapoda, Crustacea, and Hexapoda have been united in a taxon called Mandibulata. However, some molecular studies suggest a sister-group relationship of myriapods and chelicerates (together called ''Paradoxopoda'' after Mallatt et al. 2004 or ''Myriochelata'' after Pisani et al. 2004) including analyses of nuclear ribosomal genes (Mallatt et al. 2004), mitochondrial genes (Popadic et al. 1998; Hwang et al. 2001; Negrisolo et al. 2004), Hox genes (Cook et al. 2001), and 18S and 28S rRNA (von Reumont et al. 2009). The latest studies in this field analyzed the DNA sequence from 62 nuclear protein-coding genes from 75 arthropod species to reliably retrieve the Mandibulata again (Regier et al. 2010). All recent phylogenetic studies have in common that they strongly suggest a convergent conquest of land of Myriapoda and Hexapoda from a marine ancestor of Mandibulata.

The successful transition from marine to terrestrial life requires a number of physiological adaptations, for example, related to gas exchange, salt and water balance, nitrogenous excretion, thermoregulation, moulting, and reproduction (Powers and Bliss 1983; Burggren and McMahon 1988). Living on land also raises new questions regarding the evolution of chemical communication, as a transition from sea to land means that molecules need to be detected in gas phase instead of in water solution. Furthermore, the odor stimulus changes from mainly hydrophilic molecules in aqueous solution to mainly hydrophobic in the gaseous phase. How do arthropods that conquer land solve the tasks of odor detection and odor information processing, and how have the new selection pressures reshaped the sense of smell? Comparative studies between arthropod taxa that independently have established a terrestrial life style provide a powerful means of investigating the evolution of chemosensory adaptations in this environment. Studying the architecture of the olfactory system in Myriapoda and comparing it with that of Hexapoda may therefore provide insights into how the arthropod nervous system evolved in response to new environmental and ecological challenges.

Compared with hexapods and crustaceans, the architecture of the myriapod nervous system is not well understood. For *Scutigera coleoptrata* as a representative of the Chilopoda (''centipedes''), early investigations on the anatomy and microarchitecture of the nervous system include those of Saint-Remy (1887, 1889) and Hörberg (1931). Fahlander (1938) described the central nervous system of *Thereuopoda clunifer* (Scutigeromorpha). These studies showed that the deutocerebrum of Scutigeromorpha contains 2 glomerular masses. The structure of the anterior mass was described by Saint-Remy (1887, 1889) and Hörberg (1931) as irregular, ''sausage-like'', or as convoluted ribbons. In *T. clunifera*, Fahlander (1938) specified the deutocerebral lobe neuropils as numerous, dense glomerular masses that are circular in diameter. A more recent brief description of the deutocerebral neuropils of *Lithobius forficatus* (Lithobiomorpha) was given by Strausfeld et al. (1995). Some other aspect of the myriapod nervous system such as the organization of the central complex (Loesel et al. 2002) and the optic neuropils (Strausfeld 2005) as well as eye development (Harzsch et al. 2007) have received attention more recently and were analyzed against a phylogenetic background. However, little detailed information is available about the primary olfactory centers in Myriapoda. We have chosen the centipede *S. coleoptrata* (Linnaeus, 1758) for our analysis of the myriapod central olfactory pathway. This centipede is a raptorial animal that preys on living arthropods and is among the fastest moving terrestrial arthropods (Rosenberg 2009). According to the recent most phylogenetic analyses, the Scutigeromorpha are the sister group to all remaining chilopod subgroups that are summarized in the taxon Pleurostigmophora (Edgecombe & Giribet 2007; Sheer and Edgecombe 2010) and therefore sensory systems may have retained aspects that are plesiomorphic for the Myriapoda. For instance, in the optic system, it is assumed that the ommatidia of Scutigeromorpha with eucone crystalline cone cells with their nuclei placed outside the core compartments may reflect a state already present in the last common ancestor of the Mandibulata (Harzsch 2006; Müller et al. 2007). Olfaction in myriapods is almost *terra incognita,* and many questions can thus be asked: Is the nervous system suited to process olfactory signals from the antenna like in hexapods or crustaceans? Does *S. coleoptrata* respond to olfactory stimuli in behavioral experiments? In the present study, we have analyzed the architecture of the central olfactory pathway of *S. coleoptrata* and have conducted behavioral tests with prey and chemical stimuli to answer these questions.

Materials and methods

Experimental animals

Specimen of *S. coleoptrata* (Linnaeus, 1758) (Figure 1) were collected on the Balearic island Ibiza mainly in pine forests. If not fixed directly after capture, individuals were kept in plastic tubes (Falcon tubes 50 ml) at room temperature. For keeping, animals were transferred into standard *Drosophila* rearing tubes supplied with bark and water. They were fed with *Drosophila melanogaster* or juveniles of *Acheata domesticus*. Only fully adult specimens were used for experiments. Fully adult specimens have developed all 15 leg pairs and a body length of at least 20 mm (reviewed in Rosenberg 2009).

Histology

For section series, several individuals were decapitated and prefixed for 24 h in a solution of 10 parts 80% ethanol, 4 parts 37% formaldehyde and 1 part 100% acetic acid. After washing in sodium hydrogen phosphate buffer (phosphate buffered saline [PBS], pH 7.4), specimens were postfixed for 1 h in 2% OsO_4 solution (same buffer) at room temperature and, following dehydration in a graded series of acetone, embedded in Araldite (Araldite epoxy resin kit, Agar Scientific). Serial semi-thin sections (1–1.5 μm) were prepared with a Microm HM 355 S and stained using 1% toluidine blue and Pyronin G in a solution of 1% sodium tetraborate. Overall, section series of 5 specimens were investigated.

Immunohistochemistry

For immunohistochemistry, specimens were fixed for 4 h at room temperature in 4% paraformaldehyde in PBS. The isolated brains were dissected, washed 4× 30 min in PBS, embedded in agarose (Agarose Broad Range, Carl Roth), and subsequently sectioned (80 μm) with a HM 650 V vibratome (Microm). Permeabilization of the brains in PBS–TX (PBS, 0.3% Triton X-100) for 1 h at 4 °C was followed by incubation in primary antibodies overnight at 4 °C. The antisera used were polyclonal rabbit anti-FMRFamid (1:1000, DiaSorin), monoclonal mouse anti-synapsin "Synorf1" antibody (1:30 in PBS–TX, antibody provided by E. Buchner, Universität Würzburg, Germany), rabbit anti-Dip-allatostatin 1 (AST-A, 1:2000, provided by H. Agricola), and mouse anti-tyrosinated tubulin (1:1000, Sigma). After incubation in the primary antisera, tissues were washed in several changes in PBS for 2 h at room temperature and incubated in a secondary Alexa Fluor488 or secondary Alexa Fluor546 antiserum (1:50, Invitrogen) overnight at 4 °C. All sections were counterstained with the nuclear marker bisbenzimide (0.1%, Hoechst H33258) for 1 h at room temperature. Some sections were processed with a histochemical counterstain, a high-affinity probe for actin, by adding Phallotoxins conjugated to Alexa Flour546 (1:50, Molecular Probes) during the incubation in the secondary antibody. Finally, all tissues were washed for 2 h in several changes of PBS and mounted in Mowiol (Calbiochem). Overall, immunohistochemical and histochemical experiments were conducted with 15 specimens (synapsin + phalloidin $n = 5$, synapsin + RFamid $n = 5$, tyrosinated-tubulin + A-type allatostatin $n = 5$).

Figure 1 *Scutigera coleoptrata* (Linnaeus, 1758). Scale bar = 10 mm. Original kindly provided by S.Fischer. This figure appears in color in the online version of *Chemical Senses*.

Specificity of the antisera

The tetrapeptide FMRFamide and FMRFamide-related peptides are widely distributed among invertebrates and vertebrates and form a large neuropeptide family with more than 50 members all of which share the RFamide motif (reviews: Price and Greenberg 1989; Greenberg and Price 1992; Nässel 1993; Homberg 1994; Dockray 2004; Nässel and Homberg 2006; Zajac and Mollereau 2006). The antiserum we used was generated in rabbit against synthetic FMRFamide (Phe-Met-Arg-Phe-amide) conjugated to bovine thyroglobulin (DiaSorin, Cat. No. 20091, Lot No. 923602). According to the manufacturer, staining with this antiserum is completely eliminated by pretreatment of the diluted antibody with 100 μg/ml of FMRFamide. We repeated this experiment and preincubated the antiserum with 100 μg/ml FMRFamide (Sigma; 16 h, 4 °C) and this preincubation abolished all staining. We conclude that the DiaSorin antiserum that we used most likely labels any peptide terminating with the sequence RFamide. Therefore, we will refer to the labeled structures in our specimens as "FMRFamide-like immunoreactive (RFir) neurons" throughout the paper.

The monoclonal anti-tyrosine tubulin (mouse IgG3; Sigma Product Number T 9028, Clone TUB-1A2) was raised against a peptide containing the carboxy terminal amino acids of α-tubulin. According to the manufacturer, this antibody reacts with tyrosine tubulin from bovine brain, African monkey green kidney cells, dog kidney, marsupial kidney, mouse pituitary tumor (AtT-20), yeast, and *Xenopus*, indicating that the antigen that this antibody recognizes is evolutionarily conserved across a broad range of species. Tubulin is the major building block of microtubules and represents a heterodimer of α-tubulin and β-tubulin. Microtubules grow and turn over rapidly, but some populations

of interphase microtubules are more stable, such as acetylated α-tubulin (Kreis 1987). Tubulin tyrosinylation is involved in the assembly status of tubulin. Tyrosinated tubulin (tyr-tubulin) represents a relatively dynamic subclass of interphase microtubules (Kreis 1987).

The monoclonal mouse anti-*Drosophila* synapsin "Synorf 1" antibody (provided by E. Buchner, Universität Würzburg, Germany) was raised against a *Drosophila* Glutathione S-Transferase(GST)-synapsin fusion protein and recognizes at least 4 synapsin isoforms (ca. 70, 74, 80, and 143 kDa) in western blots of *Drosophila* head homogenates (Klagges et al. 1996). In western blot analysis of crayfish homogenates, this antibody stains a single band at approximately 75 kDa (Sullivan et al. 2007). In a western blot analysis comparing brain tissue of *D. melanogaster* and the terrestrial hermit crab *Coenobita clypeatus*, the antibody provided identical results for both species, staining 1 strong band around 80–90 kDa and a second weaker band slightly above 148 kDa (Harzsch and Hansson 2008). Furthermore, the antibody consistently labels brain structures in representatives of malacostracan crustaceans (Beltz et al. 2003; Vilpoux et al. 2006; Harzsch and Hansson 2008) in a pattern that is consistent with the assumption that this antibody does in fact label synaptic neuropil in Crustacea. We also conducted a western blot analysis comparing brain tissue of *D. melanogaster* and *S. coleoptrata*. The antibody provided similar results for both species staining 1 strong band around 80–90 kDa. Our analysis strongly suggests that the epitope that Synorf 1 recognizes is strongly conserved between the fruit fly and the chilopod. Beyond the arthropods, this antibody even labels synaptic neuropil in ancestral taxa of protostomes such as the Chaetognatha (Harzsch and Müller 2007; Rieger et al. 2010) and Plathelminthes (Cebia 2008) suggesting that the epitope that this antiserum recognizes is highly conserved over wide evolutionary distances.

Allatostatin peptides share the conserved C-terminal sequence -YXFGL-amide (Bendena et al. 1999) and are present in the nervous system of various insects analyzed so far (reviewed in Kreissl et al. 2010). In hexapods, allatostatins are often colocalized with other transmitters, for example with γ-aminobutyric acid (GABA) and other peptides in antennal lobes of moths (Berg et al. 2007, 2009). Corelease with GABA is likely related to the inhibitory function of AST. The antiserum against *Diploptera punctata* (Pacific beetle cockroach) A-type allatostatin I (Dip-allatostatin I, APSGAQRLYGFGL-amide) was provided by H. Agricola (Friedrich-Schiller Universität, Jena, Germany). Vitzthum et al. (1996) have characterized the Dip-allatostatin I antibody. It recognizes all Dip-allatostatins. No cross-reactivity was found with corazonin, crustacean cardioactive peptide (CCAP), FMRFamide, leucomyosuppression, locustatachykinin 11, perisulfakinin, and proctolin as tested by noncompetitive enzyme-linked immunosorbent assay. Vitzthum et al. (1996) showed that preadsorption of the diluted antisera against Dip-allatostatin I, GMAP, and *Manduca sexta* allatotropin with 10 μM of their respective antigens abolished all immunostaining in brain sections of *Schistocerca gregaria*. We performed a preadsorption test and preincubated the antiserum with 200 μg/ml A-type allatostatin I (Sigma, A9929; 16 h, 4 °C), and this preincubation abolished all staining. We conclude that the antiserum that we used most likely labels any peptide terminating with the sequence YXFGL-amide. Therefore, we will refer to the labeled structures in our specimens as "allatostatin A–like immunoreactive (ASTir) neurons" throughout the paper.

Antennal backfills

For anterograde antennal backfill stainings, specimens were immobilized by slowly cooling down and mounted in plastic Petri dishes. The left antenna was then cut, leaving a stump of approximately 3 mm. A glass capillary filled with 2% Dextran-biotin (dextran, biotin, 3000 MW, lysine fixable; Molecular Probes, Cat. No. D-7135) dissolved in aqua dest. was placed over the antennal stump. Animals were kept alive for 4 h at room temperature, then decapitated and the head subsequently fixed in 4% paraformaldehyde in PBS for 4 h at room temperature. Thereafter, brains were dissected out in PBS and either processed as whole mounts or sectioned (80 μm). Vibratome sections and brains were washed 3× 20 min in PBS and incubated for 8 h in Streptavidin conjugated to Alexa 488 (1:2.500 in PBS, Molecular Probes Cat. No S-11223) over night at 4 °C. The sections and brains were then rinsed 3× 20 min with PBS and finally mounted in Mowiol. We performed 5 successful backfills all of which yielded a homogeneous representation of primary sensory neuropils with only little variation between the structural patterns.

Golgi impregnation

Heads of *S. coleoptrata* were prefixed in a solution containing 5 parts 2.5% potassium dichromate, 1 part 25% electron microscopy-grade glutaraldehyde and 3% glucose for 4 days at 4 °C. After dissection, brains were washed in 2.5% dichromate for 1 h, followed by 4 days incubation in 99 parts 2.5% potassium dichromate and 1 part 1% osmium tetroxide, and then immersed in 0.75% silver nitrate. Finally, brains were dehydrated through a graded series of ethanol and propylene oxide and embedded in Durcupan (Fluka Chemicals), which was polymerized over 2 nights at 60 °C. Serial 30 μm sections were cut with a sliding microtome (Jung HN 40 and Leica SM 2000R). For details on the method, see Strausfeld (1980).

Microscopy

Whole mounts and brain sections were viewed with a Zeiss AxioImager equipped with the Zeiss Apotome structured dillumination device for optical sectioning. Digital images were processed with the Zeiss AxioVision software package. In addition, specimens were analyzed with a laser scanning microscope (Zeiss 510 Meta) using 10× (Zeiss EC

Plan-Neofluar 10×/0.3) and 20× (Zeiss Plan-Apochromat 20×/0.8) objectives. Double-labeled specimens were generally analyzed in the multitrack mode, in which the 2 lasers operate sequentially. Narrow band pass filters were used to assure a clean separation of the labels and to avoid cross-talk between the channels. Images based on *Z*-stacks of several optical sections were obtained using the LSM 510 SP2 Software (Zeiss). All images were obtained at 1024 × 1024 pixel resolution and processes in Adobe Photoshop using global contrast and brightness adjustment features.

Three-dimensional reconstruction

For the alignment and 3-dimensional (3D) reconstruction, AMIRA 4.1 (Mercury Systems) operated on a FS Celsius work station was used. In each section, contours of the neuropils were demarcated and a 3D model, in which individual neuropils could be defined, was generated. Reconstructions from antennal backfills were generated by using the Isosurface function. A nomenclature of the olfactory subunits was developed based on the general position of single neuropils in the deutocerebrum, where capital letters give the position: anterior (A), posterior (P), ventral (V), dorsal (D), and central (C).

Ethological experiments

To test whether *S. coleoptrata* is able to detect airborne stimuli, an ethological test was designed. Two holes (1 cm in diameter) were drilled into the bottom of a plastic box (25 × 20 × 8 cm) in opposite quadrants (Figure 9A). Two round containers with a height of 5 cm were placed underneath the holes, one of them containing a stimulus. As stimuli, living juvenile crickets (*A. domesticus*) or an extract of the same species was presented. To produce the extract, 50 juvenile specimens of *A. domesticus* were immersed in 1 ml methylene chloride for 1 h at room temperature in darkness. The decanted liquid was dried with sodium sulfate decahydrate and concentrated under a light nitrogen stream to 100 µl. Ten microliters (the equivalent to 5 living juvenile specimens) were then pipetted onto a filter paper (10 × 5 mm) that was placed in one of the containers. Specimens were tested individually in the arenas. The position of the stimulus was changed randomly between the experiments. After the experiment, all arenas and handling containers were cleaned, rinsed in aqua dest., and dried.

The behavioral experiments were conducted over night in darkness starting round 10.00 PM. Single individuals were placed in individual arenas, which were then inspected on the following morning. A positive choice was recorded when *S. coleoptrata* had moved into one of the containers. Otherwise, the trial was recorded as "no choice." Five-to-ten specimens of *S. coleoptrata* were tested per night, and new specimens were used for each replicate. The choices were analyzed with a binominal test to investigate whether the distribution of the choice differed from 50:50. Individuals that did not make a choice were excluded from statistical analyses.

In addition, a field experiment was conducted on the island of Ibiza using a glass terrarium (50 × 30 × 25 cm) in the field with the same substrate and physical conditions as the surrounding area (Figure 9B). Three filter papers (10 × 5 mm) were placed in the center of the terrarium at a distance of 5 cm to each other and impregnated with 1) 10 µl cricket extract or 2) 10 µl water. The third paper served without any impregnation as a control. Five specimen of *S. coleoptrata* were placed into the terrarium. The experiments were run during 3 nights from about midnight until about dawn. The terrarium was filmed in the dark with a Sony DCR-SR70 equipped with night shot optics and infrared illumination. The videos obtained were evaluated using VLC media player. In the video presented as Supplementary material online, the stimulus is to the left, the control in the middle, and the water-soaked paper to the right.

Results

Overview of the *Scutigera coleoptrata* brain

A dorsal to ventral series of vibratome sections reveal that the head of *S. coleoptrata* is densely packed with musculature (Figure 2). The brain is sandwiched between an anteriorly located system of muscles and more posteriorly located musculature that operates the mouthparts (Figure 2A,B). The protocerebrum expands as a huge mass dorsally to the deutocerebrum (Figures 2A,B,C and 3A; terminology according to the body axis). The well-developed elongated optic lobes extend laterally from the protocerebrum toward the compound eyes (Figure 2B,C). They comprise 2 neuropils, the distal of which is the lamina and the proximal is called medulla (Melzer et al. 1996) or visual tectum (Strausfeld 2005). The mushroom bodies or corpora pedunculata are located in the dorsal protocerebrum (Figure 7A). The deutocerebrum is the most anterior part of the brain with regard to the body axis but is located ventroposteriorly to the protocerebrum with respect to the neuraxis (Figure 3A). It receives input from the robust antennal nerves at its frontolateral edges (Figures 2E,F and 3A). These nerves, on entering the brain, divide into 2 branches: a dorsoventral part innervates the anterior neuropils (olfactory neuropils; ONs), whereas the ventrocaudal part innervates a posterior neuropil (corpus lamellosum [CL]). As in hexapods, the deutocerebrum is partitioned into many discrete neuropil units that are targeted by antennal OSN axons (Figure 3). Because of their shape, we suggest to call them olfactory neuropils (ON) rather than glomeruli or glomerular masses/neuropils. The sum of the ONs we call antennal lobe as in the Hexapoda. A demarcation between the deutocerebrum and tritocerebrum is not

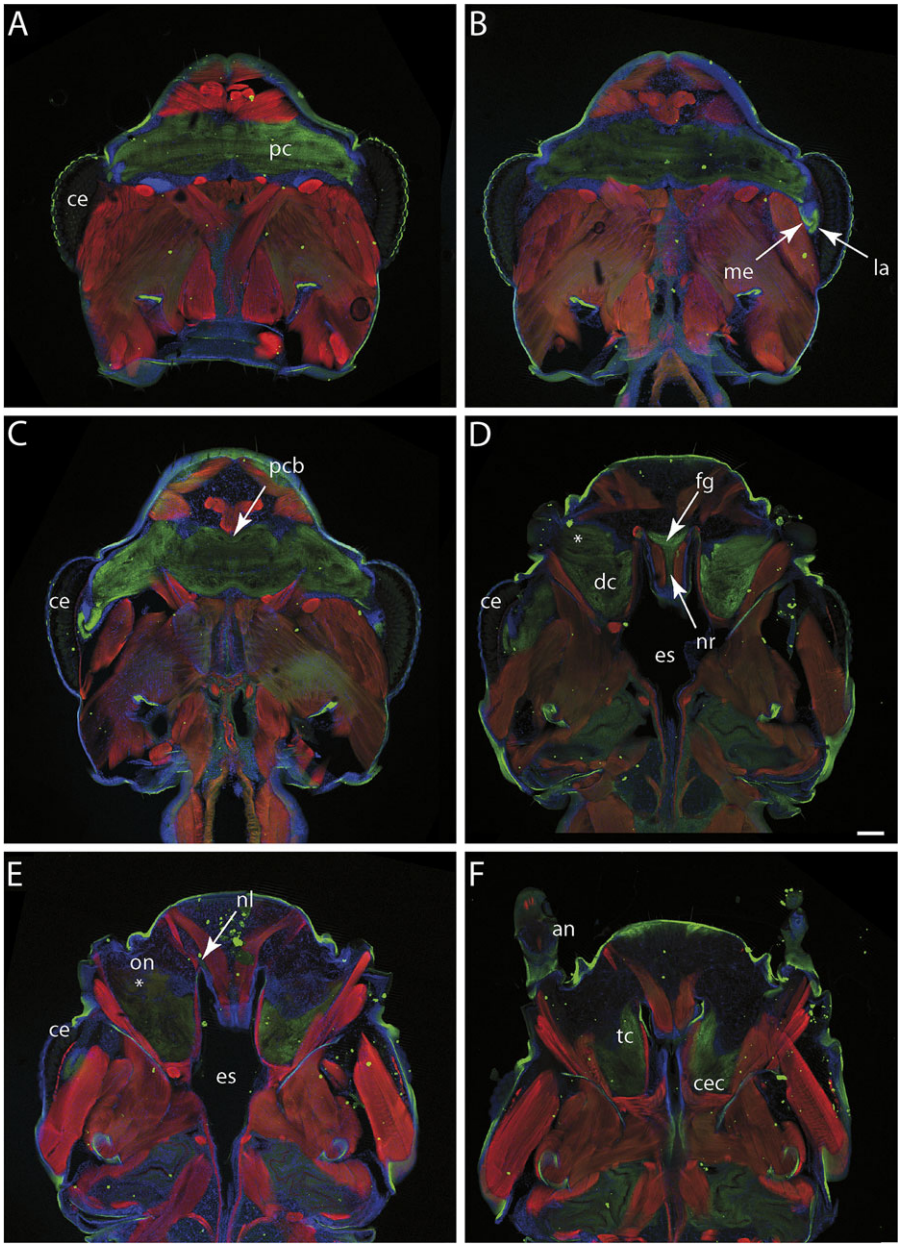

Figure 2 Selected sections from a horizontal vibratom section series through the head of *Scutigera coleoptrata* from dorsal to ventral (epifluorescence microscopy combined with the Zeiss Apotome structured illumination technique for optical sectioning); synapsin immunoreactivity and histochemical labeling of f-actin and nuclei. **(A)** Dorsal section showing compound eyes and the dorsal part of the protocerebrum. **(B)** Region of the midline neuropil. In the lateral protocerebrum, the optic neuropils lamina and medulla are visible. **(C)** Optic neuropils and protocerebral bridge. **(D)** Medial section through the deutocerebrum. The antennal nerve enters the brain and single ONs are detectable (asterisk). The frontal ganglion with the frontal connectives and the *nervus recurrens* are also visible. **(E)** Ventral section of the deutocerebrum and tritocerebrum. Single ONs are detectable (asterisk). The *nervi labrales* are visible in a mediofrontal position. **(F)** Ventral section showing tritocerebrum and circumesophageal connectives. The base of the antenna is visible. an, antenna; ce, compound eye; cec, circumesophageal connective; dc, deutocerebrum; es, esophagus; fg, frontal ganglion; la, lamina; me, medulla; nl, nervus labralis; nr, nervus recurrens; pc, protocerebrum; pcb, protocerebral bridge; tc, tritocerebrum. Scale bar for all images = 100 μm. This figure appears in color in the online version of *Chemical Senses*.

apparent, although the frontal connectives indicate the anterior margin of the tritocerebrum, just posteroventral to the deutocerebral lobes (Seifert 1967). The frontal connectives of the tritocerebrum project slightly caudally and converge medially at the frontal ganglion (Figures 2D and 3A). The *nervus recurrens* extends dorsally of the frontal ganglion on top of pharynx and esophagus (Figures 2D and 3A). A pair of labral nerves emerges in the front of the tritocerebrum (Figures 2E and 3A). These nerves converge and innervate the musculature of the clypeolabral region and the buccal gland. Paired connectives leave the tritocerebrum posteriorly to link it with the subesophageal ganglion.

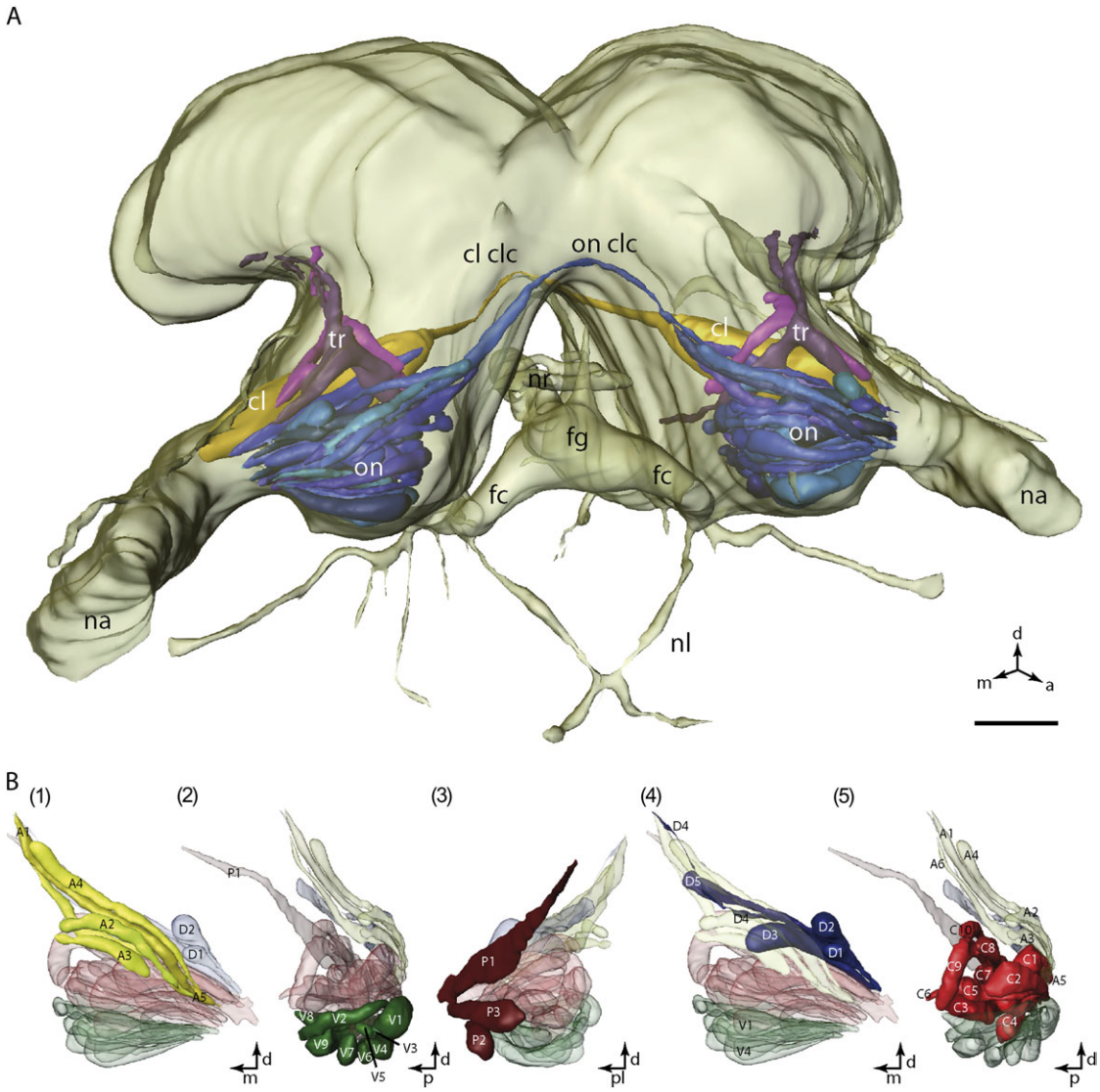

Figure 3 3D reconstructions of the brain and deutocerebral neuropils of *Scutigera coleoptrata* from a histological section series. **(A)** Reconstruction of the brain with the nerves of the deuto- and tritocerebrum. **(B)** Reconstruction of the ONs in various views (frontal, 45° angle frontal, 45° angle cranial). Color coding of neuropil groups: anterior (1), ventral (2), posterior (3), dorsal (4), and central (5). a, anterior; d, dorsal; fc, frontal connective; fg, frontal ganglion; m, median; na, nervus antennalis; nl, nervus labralis; nr, nervus recurrens; on, olfactory neuropils; p, posterior; pl, posteriolateral. Scale bar = 100 µm. This figure appears in color in the online version of *Chemical Senses*.

Backfill experiments

By backfilling the antennal nerve with anterograde axonal markers, we obtained reliable information concerning the innervation pattern of the deutocerebral neuropils. Based on these preparations, we were able to verify that antennal input does in fact target the deutocerebral lobe neuropils, which therefore are first order processing areas in the deutocerebrum. In a fill of the left antennal nerve (Figure 4A,B), the label was transported not only into the deutocerebral lobe but also along tracts projecting into the ventral protocerebrum and into the subesophageal ganglion (arrowheads in Figure 4B,C,D). The afferents separate into 2 tracts, one of which innervates the ONs, whereas the other targets the corpus lamellosum (cl; Figure 4B). These backfills also revealed contralateral connections of both the ONs and the CL (on clc and cl clc; Figure 4B). The isosurface reconstruction (Figure 5A,B) shows the 3D arrangement of this LSM section (108.7 µm from 142 optical sections). The front view displays (Figure 5A) a subset of ONs. The back view (Figure 5B) shows the architecture of the corpus lamellosum with projecting inner lamellae and the anterior closed outer lamellae (ol).

The olfactory neuropils

The dextran-biotin backfills reveal that single ONs have an elongated shape and are arranged in a parallel array

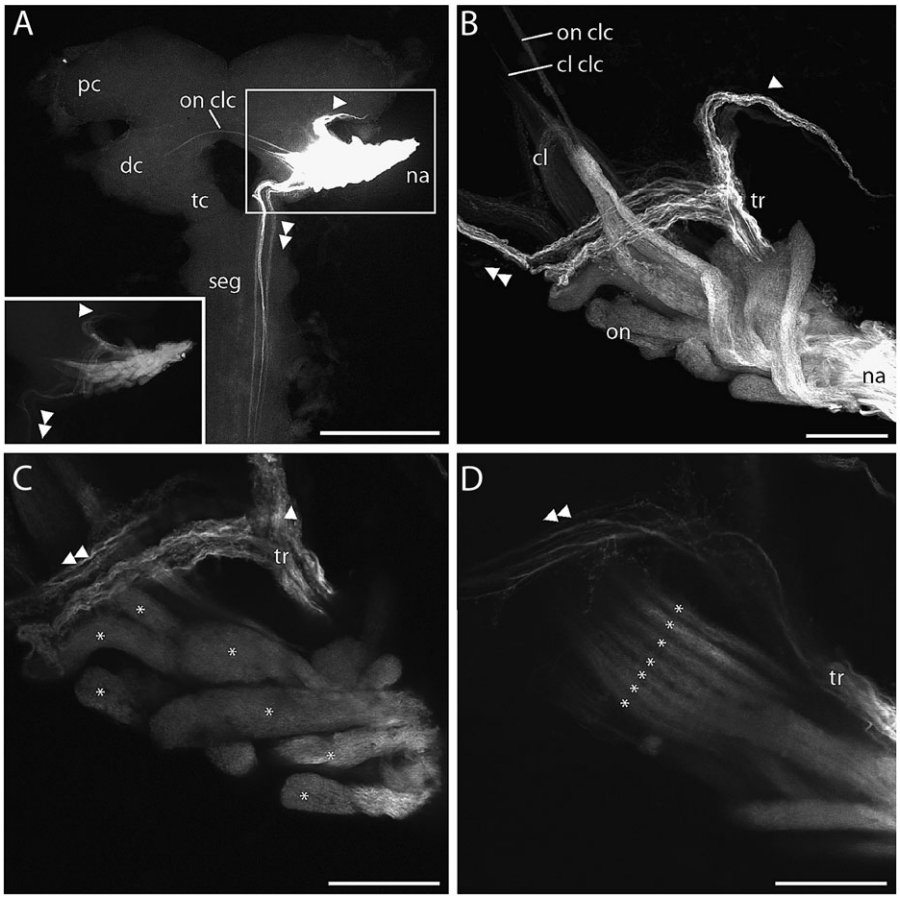

Figure 4 Dextran-biotin backfill of the left antennal nerve, all pictures were taken from the same preparation. **(A)** Epifluorescence microscopy combined with the Zeiss Apotome structured illumination technique for optical sectioning image. Whole-mount preparation of the *Scutigera coleoptrata* brain. Neuropils, contralateral connection of ONs, and projecting tracts (arrowheads) are labeled. The inset shows labeled projections from the antennal nerve (streptavidin). **(B)** Higher magnification of the dextran-biotin backfill of the left deutocerebral lobe. Projection of a confocal stack with 142 single images covering a total thickness of 108.7 μm. Filled neuropils with on clc and cl clc are visible. The base of projecting tr is not visible, nevertheless, the bifurcation into dorsal (arrowhead) and ventral (double arrowhead) tract is detectable. Posterior tracts and corpus lamellosum are weaker stained in this view. **(C)** Single optical section (0.76 μm) of ONs (asterisks) and distal bifurcation of projecting tracts. **(D)** Single optical section (0.76 μm) of the corpus lamellosum. Seven single lamellae are detectable (asterisks). The proximal region of projecting tracts is visible. cl, corpus lamellosum; cl clc, contralateral connection of the corpus lamellosum; dc, deutocerebrum; na, nervus antennalis; on, olfactory neuropils; on clc, contralateral connection of the olfactory neuropils; pc, protocerebrum, tc, tritocerebrum; tr, tracts. Single arrowheads: dorsal projecting tracts and double arrowheads: ventral projecting tracts. All scale bars 100 μm.

(Figure 4C, asterisks). Synapsin immunoreactivity provides a good overview over the general architecture of the ONs and confirms their elongated shape (Figure 6B,C). In horizontal vibratome sections of the whole head, a slight medioposterior direction of the ONs is visible (asterisks in Figure 2D,E). A projection of 43 single confocal images (covering ca. 32 μm) shows that the neuropil of the ONs is densely and uniformly stained (Figure 6B, frontal view). A comparison of the backfill data (Figure 4B,C) with the Synapsin immunoreactivity (Figure 6B) suggests that the antennal afferents extend throughout the entire ONs to establish synaptic connections with interneurons. Not only in a different immunohistochemical preparation (Figure 6C) but also in histological sections (Figure 6F), the neuropil of the ONs appear compact without subcompartments.

The shape and arrangement of the ONs were reconstructed from histological section series stained with toluidine blue, where single neuropils appear highly contrasted (Figure 6F). The roughly parallel array of ONs emerges from the entry point of the antennal nerve and extends in a mediodorsal direction. The 3D reconstruction of the ONs show that they are arranged in a bilaterally symmetrical pattern (Figure 3A), so that it is possible to match the corresponding ONs in the left and right antennal lobe. In 3 histological series from different specimens, we consistently found 34 distinct and uniquely identifiable ONs in a more or less invariant arrangement that seems to be fixed in the 3D space within the deutocerebrum (Figure 6A). This set can be subdivided into 5 groups according to their position: an anterior group (A1–A6, Figure 3B), a ventral group (V1–V9), a posterior group (P1–P3), a dorsal group (D1–D5), and a central

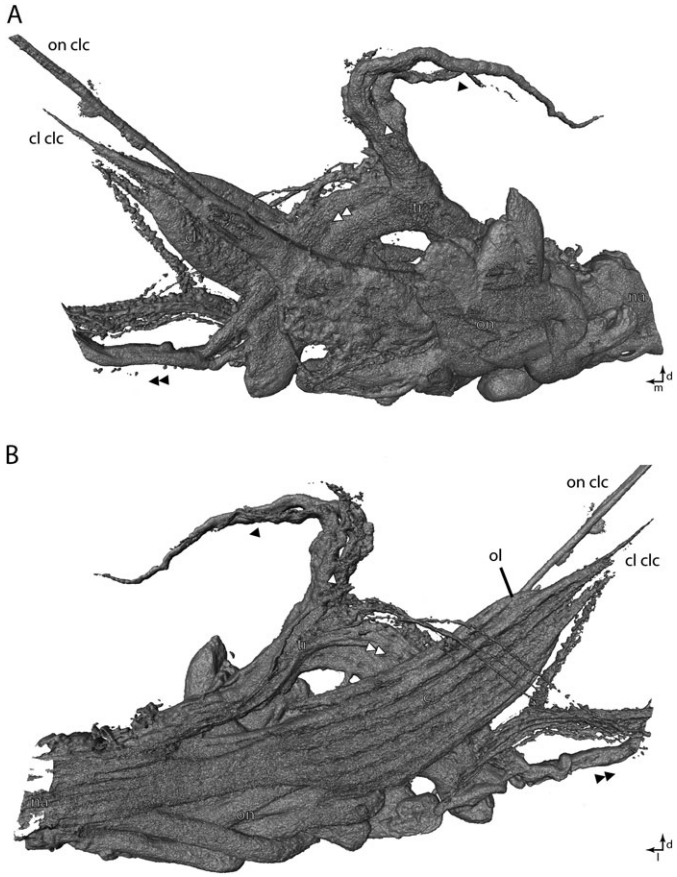

Figure 5 3D isosurface reconstruction of the dextran-biotin backfill shown in Figure 4 from a confocal stack with 142 single images covering a total thickness of 108.7 μm. Filled neuropils with contralateral connections of ONs and corpus lamellosum are visible. **(A)** Front view. **(B)** Back view. The base of projecting tracts is visible dorsal of the base of the corpus lamellosum as well as the bifurcation into dorsal (arrowhead) and ventral (double arrowhead) tr. cl, corpus lamellosum; cl clc, contralateral connection of the corpus lamellosum; d, dorsal; l, lateral; m, median; na, nervus antennalis; ol, outer lammelae of the corpus lamellosum; on olfactory neuropils; on clc, contralateral connection of the olfactory neuropils; tr, tracts.

group (C1–C11). The 2 uppermost ONs (A1, A6) extend into a mediodorsal direction toward the midline whereas the more ventral ones are shorter (Figure 3, groups V, C). The distal end of these ventral ONs is often thickened and/or bent posteriorly (Figure 3B, e.g. V2, C2). The ONs have a length of around 250–400 μm. The cross-sectional profile is more or less 35 μm in diameter. Volume measurements range from approximately 15 500 μm^3 (ON D4) to approximately 1 030 000 μm^3 (ON C3). In average, an ON has a volume of approximately 443 500 μm^3, and the sum of all neuropils is 15 080 000 μm^3.

Localization of RFamide-like immunoreactivity (RFir) reveals mostly fibers that surround the ONs diffusely, the associated somata being located in a mediolateral position to the ONs (arrows in Figure 6E 1 and 2). The ONs exhibited weak RFir (Figure 6E 1 and 2). Allatostatin-like immunoreactivity (ASTir) is expressed more strongly in the deutocerebral lobes (Figure 6D), where a distinct signal is present within the ONs (inset Figure 6D). Twenty to 30 ASTir neurons are located anteriorly to the ONs. Most likely, these neurons give rise to the plexus of immunolabeled fibers in the central area of the neuropils that form distinct synaptic endings. These endings are evenly distributed throughout the neuropil and do not show any regional concentrations.

Golgi impregnations provide information about the morphology of single neurons and, when impregnated in quantity, their contributions to the neuroarchitecture of defined synaptic neuropils. Due to the fact that the Golgi method does not reveal the entire array of neurons, only a subset of axons is visible. Large neurons are often partially impregnated, particularly when several occur together. The neuropils themselves can be resolved as delineated volumes that show up darker than the surrounding tissue even when no neuronal processes have been impregnated. This staining property reveals the 2 kinds of neuropils in the deutocerebrum: the corpus lamellosum (Figure 8A, cl) and the smaller ONs (Figure 8A, on). On entering the brain, axons from the antennal nerve project into a kind of sorting zone from where they follow distinctive trajectories either into the ONs or into the CL (Figure 8A,B). Afferents targeting the ONs are much thinner than those that extend into the CL (Figure 8A,C). Within the ONs, afferent neurons form bundles with more or less parallel neurites (Figure 8C,D,E). Each axon is decorated with numerous bouton-like swellings, here interpreted as presynaptic specializations (arrows in Figure 8D). Larger processes, interweaving among these endings, may belong to local interneurons and, or, relay neurons. Their axons are equipped with distinct synaptic swellings. They branch intensely in the ONs with their synaptic fields overlapping those of the OSN axons (Figure 8D,F). The terminals in ONs are tangled, have many branches, and are generally of very small diameter (Figure 8E).

Corpus lamellosum

The ventrocaudal part of the antennal nerve innervates a presumed mechanosensory neuropil called the corpus lamellosum (CL) that is composed of approximately 8 thin neuropils arranged in parallel, called lamellae (asterisks Figure 4D). Volume measurement of 1 CL revealed a size of approximately 7 900 000 μm^3. Golgi impregnations show that while the OSNs targeting the ONs appear thin, the axons targeting the CL are much thicker (Figure 8A,C) and give off short side branches along their length (Figure 8A,B,C). In histological sections, the neuropil of the CL stands out in high contrast so that the subdivision into the lamellae is clearly recognizable (Figure 7E). Two different types of lamellae are present. The outer lamella medially forms a 180° loop (ol in Figure 7B, arrow in Figure 7 C1, E), whereas the inner lamellae (il in Figure 7B) extend further dorsomedially to project toward the contralateral side. These projections connect to the heterolateral neuropil and form the posterior

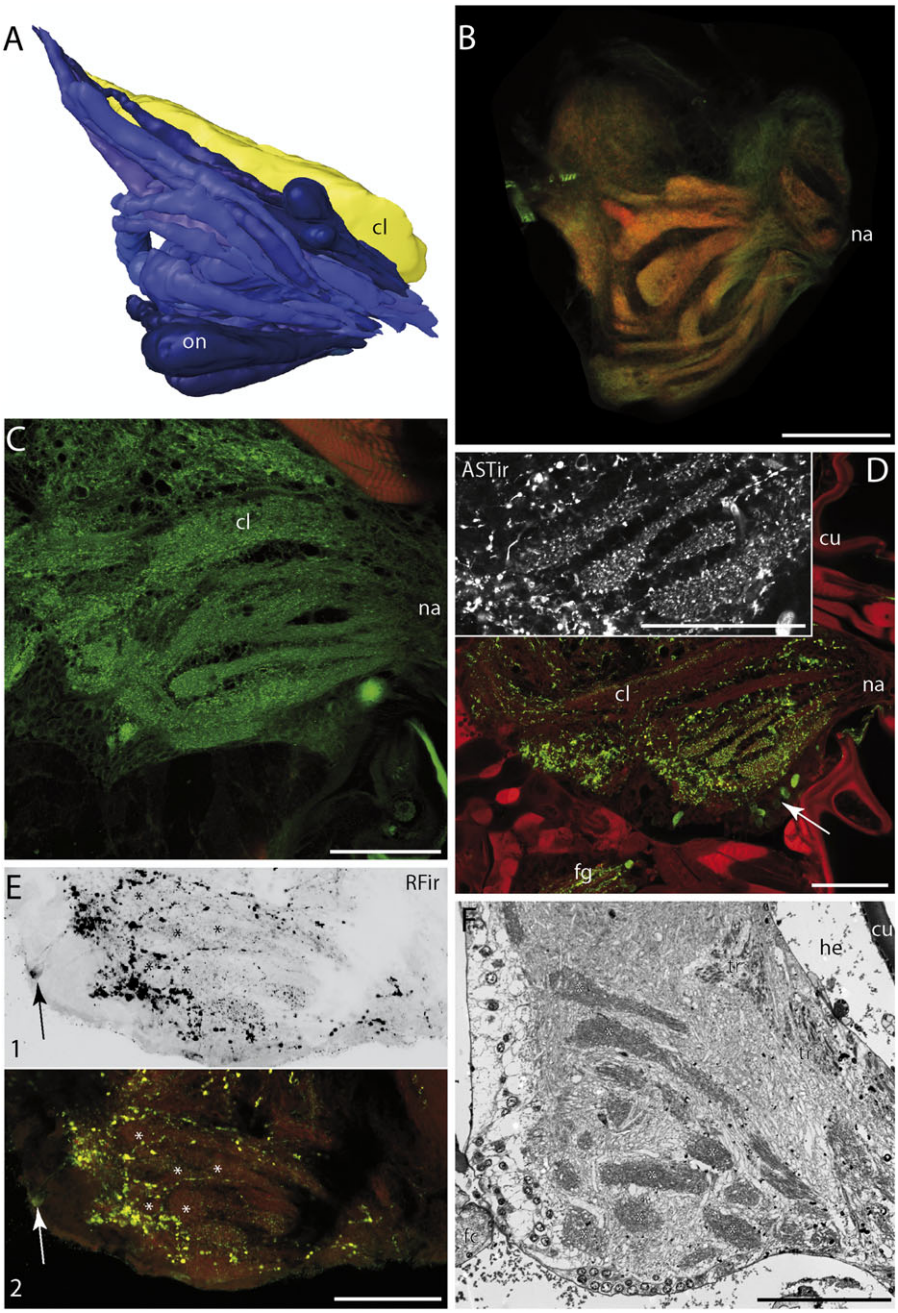

Figure 6 ONs visualized with different methods. **(A)** The 3D reconstruction of the 34 ONs and the corpus lamellosum of one deutocerebral lobe based on a histological section series (frontal view). **(B)** Synapsin immunoreactivity and phalloidin labeling. Medial frontal section of the left antennal lobe. Projection of 43 optical sections covering a thickness of 31.8 μm. **(C)** Single optical section of synapsin immunoreactivity and phalloidin labeling in the left antennal lobe (80 μm horizontal vibratome section). **(D)** Immunolocalization of tubulin and ASTir, single optical section of a 80 μm horizontal vibratome section. Inset shows ASTir in the ONs. ASTir somata are located in front of the ONs (arrow). **(E)** Single optical section of a 80 μm vibratome section of the left antennal lobe (frontal view). 1: Black–white inverted RFir. Arrow identifies 2 medial RFir somata, and asterisks mark single ONs. 2: Synapsin immunoreactivity and RFir. **(F)** Histological cross section (1.5 μm) of the left deutocerebral lobe. Asterisks show selected single ONs. Tangential aspects of projecting tracts are visible in the upper right quadrant. Lower left: tangential section of a frontal connective. cl, corpus lamellosum; cu, cuticle; he, hemolymph; fc, frontal connective; fg, frontal ganglion; na, nervus antennalis; pc, protocerebrum. All scale bars = 100 μm. This figure appears in color in the online version of *Chemical Senses*.

antennal commissure (Figures 3A and 4B, arrow in Figure 7A). Phalloidin histochemistry highlights additional structural features. In a stacked frontal projection of optical sections (Figure 7B), the lamellae are clearly visible. Single sections of this stack (Figure 7C) depict 3 sequential views from anterior to posterior, where the 2 different types of lamellae and the contralateral projections are visible. Phalloidin histochemistry reveals 8 lamellae (Figure 7 asterisks in C2), whereas

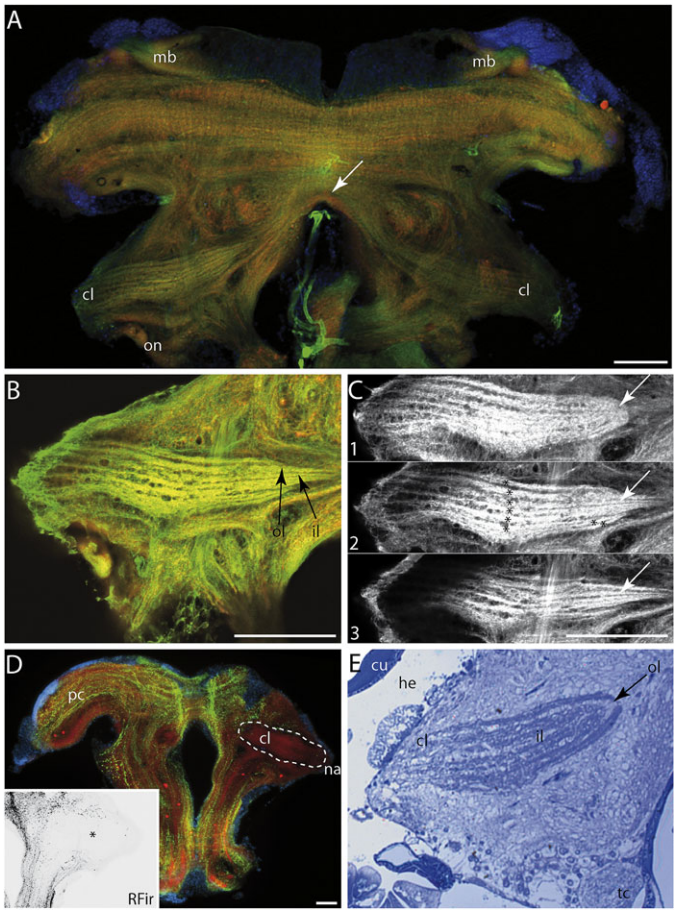

Figure 7 The corpus lamellosum visualized with different methods. **(A)** Epifluorescence microscopic image of the brain (80 µm vibratom cross section) combined with the Zeiss Apotome structured illumination technique for optical sectioning showing synapsin immunoreactivity, phalloidin labeling, and nuclear labeling. Arrow identifies the thin contralateral connection of the neuropil. **(B)** Projection of a confocal stack of 37 single sections covering a thickness of 27.3 µm of the right corpus lamellosum showing synapsin immunoreactivity and phalloidin labeling. The connection of the outer closed lamella is not visible in this view. **(C)** Single optical sections of the projection shown in (B). 1: Anterior section with closed outer lamella. 2: Middle section with outer lamella covered by projecting inner lamellae. In this view, 8 single lamellae are visible (asterisks). 3: Posterior section with projecting inner lamellae. **(D)** Epifluorescence microscopic image of a 80 µm vibratom section combined with the Zeiss Apotome structured illumination technique for optical sectioning showing synapsin immunoreactivity, phalloidin labeling, and nuclear labeling. The region of the corpus lamellosum is marked and no further partitions in the synapsin immunoreactivity are visible. Inset: RFir of the same preparation (black–white inverted). Asterisk marks the position of the corpus lamellosum. **(E)** Histological cross-section (1.5 µm) of the right deutocerebral lobe. The closed outer lamella and inner lamellae are highly contrasted. cl, corpus lamellosum; cu, cuticula; he, hemolymph; il, inner lamellae; mb, mushroom body; ol, outer lamella; on, olfactory neuropils; pc, protocerebrum; tc, tritocerebrum. All scale bars = 100 µm. This figure appears in color in the online version of *Chemical Senses*.

backfilling experiments show 7 lamellae (Figure 4D). Immunolocalization of RFamide-like peptides does not reveal any signal in the CL (inset Figure 7D). However, allatostatin-like immunoreactivity is present in the CL but in a lower intensity as in the ONs (Figure 6D). Only the posterior area was labeled with this antiserum whereas the more anterior area displays only a loose, punctual distribution of label.

Behavioral experiments

When choosing between the containers with live crickets (stimulus) and the empty one (control), individuals of *S. coleoptrata* with a high significance preferred the crickets. The ratio stimulus versus control for all experiments conducted was 36:12 ($n = 48$) (binominal test $P < 0.001$). When presenting the cricket extract, the centipedes also robustly preferred the stimulus over the control (Figure 9). The ratio stimulus versus control for these experiments was 33:14 ($n = 47$) (binominal test $P < 0.005$).

In experiments under controlled field conditions, we could distinguish 2 different behavioral patterns with regard to the samples that we presented: undirected walking over the sample versus arrestment. "Undirected" behavior was defined as a rapid movement over the filter paper, whereas for an "arrestment" behavior the animals had to halt at the filter paper for at least 3 s. Over 3 nights and duration of nearly 15 h, 39 contacts with the exposed filter papers were observed. Undirected behavior was recorded for 20 contacts, 6 times at the stimulus, 8 times at the control, and 6 times at the water-soaked paper. Arrestment behavior was exclusively recorded at the stimulus and took place 19 times. Overall, 25 visits at the stimulus were recorded. Numbers of contacts on the stimulus were significantly higher than on control and water (Kruskal–Wallis test $P < 0.001$). The Supplementary online video shows a compilation of the 9 contacts that took place during the first night of experiments. In this video, the stimulus is to the left, the control in the middle, and the water-soaked paper to the right. Scenes 1, 3, 5, 6, 8, and 9 show arrestment behavior at the stimulus. It has to be noted that these scenes were recorded in darkness under infrared light illumination. In scenes 5, 6, and 9, the animals can be seen to slowly approach the stimulus in a directed way. Upon reaching the filter paper, the animals abruptly halt and begin to inspect the paper with their mouthparts and anterior limbs. After a few seconds, the animals seem to lose interest and wander off.

Discussion

The deutocerebrum of *Scutigera coleoptrata*

The nervous system of Scutigeromorpha was first investigated in the late 19th century by Saint-Remy (1887, 1889) and the beginning of the 20th century by Hörberg (1931). Fahlander (1938), in a broad comparative study, described the nervous system of various Chilopoda and also interpreted the results from Saint-Remy and Hörberg. All 3 authors found that the deutocerebrum contains glomerular neuropils that can be divided into 2 different classes. However, although all 3 authors mentioned elongated neuropils

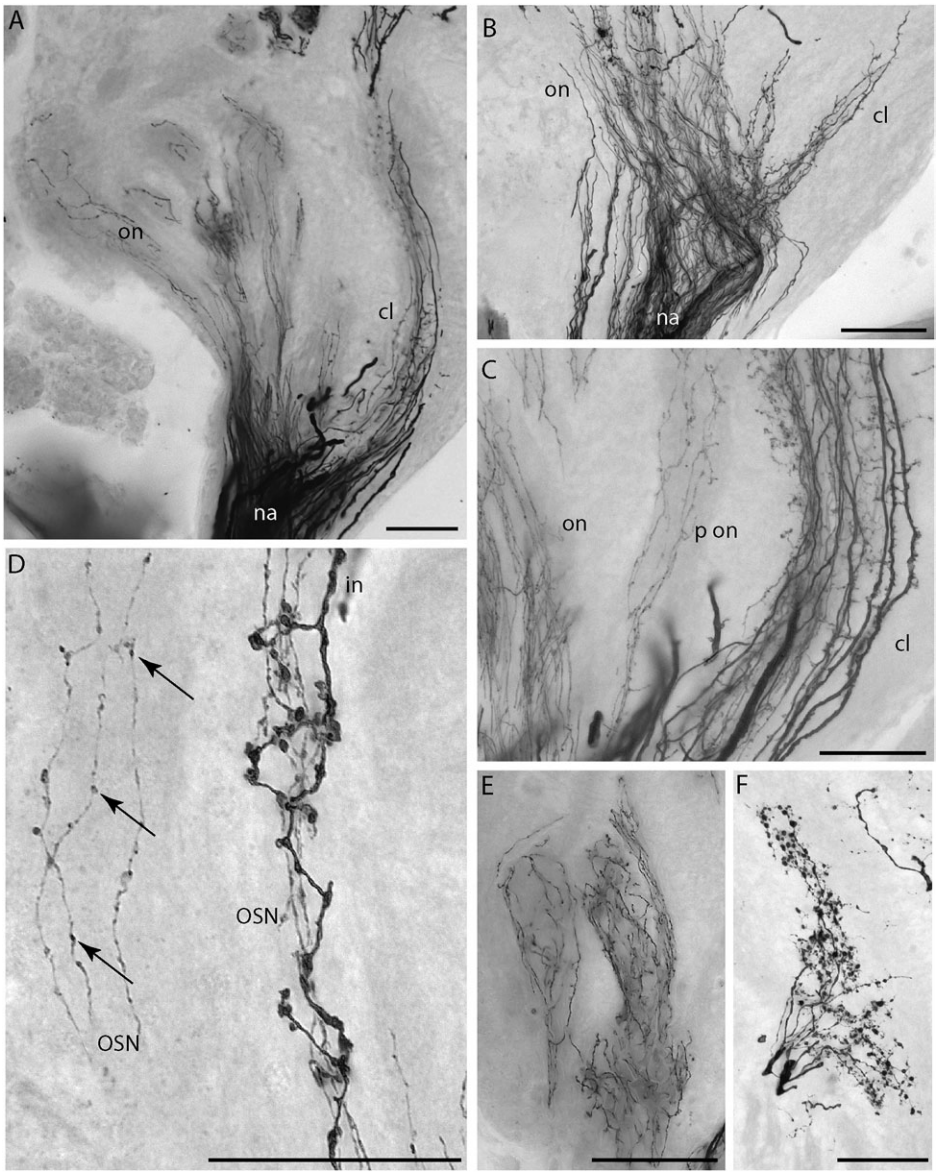

Figure 8 Horizontal sliding mictrotome sections (30 μm) of Golgi impregnated brains of *Scutigera coleoptrata*. **(A)** Penetration of afferent axons into the ONs and the corpus lamellosum. Scale bar = 100 μm. **(B)** Sorting zone of OSNs and mechanosensory axons. Orientation into the more or less parallel arrangement of OSNs. **(C)** Left: parallel axons target the ONs. A posterior ON is innervated by single neurites. Right: Innervation of the corpus lamellosum. Fine lateral and medial branchings are visible. **(D)** Left: thin and parallel OSNs targetting an ON. Arrows mark putative presynaptic buttons. Right: Secondary thicker axon (probably belonging to an interneuron) with putative postsynaptic buttons. **(E)** Arrangement of OSNs in 2 ONs. **(F)** Secondary neuron (presumably interneuron) projects with longitudinal spreading ramifications on an ON. Scale bars in (B–F) = 50 μm.

in the antennal lobe, their number and structural composition remained unclear. Fahlander (1938) described an anterior antennal commissure but overlooked that this structure is actually formed by the extensions of at least 2 neuropils (neuropils A1 and D4 in the present report). By comparing histological section series of different specimens and performing immunohistochemical and tracing experiments, we reconstructed a map of 34 individually identifiable ONs in the antennal lobe of *S. coleoptrata.* This map is fairly invariant between specimens considering number, position and shape of the ONs. Such an invariant arrangement resembles the array of olfactory glomeruli mapped in different hexapod species (e.g., Chambille and Rospars 1981; Rospars 1983; Rospars and Hildebrand 1992; Galizia et al. 1999; Laissure et al. 1999; Berg et al. 2002; Huetteroth and Schachter 2005; Kirschner et al. 2006; Ghaninia et al. 2007; Zube et al. 2008; Dreyer et al. 2010). In Fahlander's (1938) schematic presentation of the *Thereuopoda clunifera* (Scutigeromorpha) brain, he depicted 2–3 elongated neuropils innervated by the antennal nerve and two neuropil masses in the distal region leading to the anterior antennal commissure. Our data reveal that in *S. coleoptrata* there are

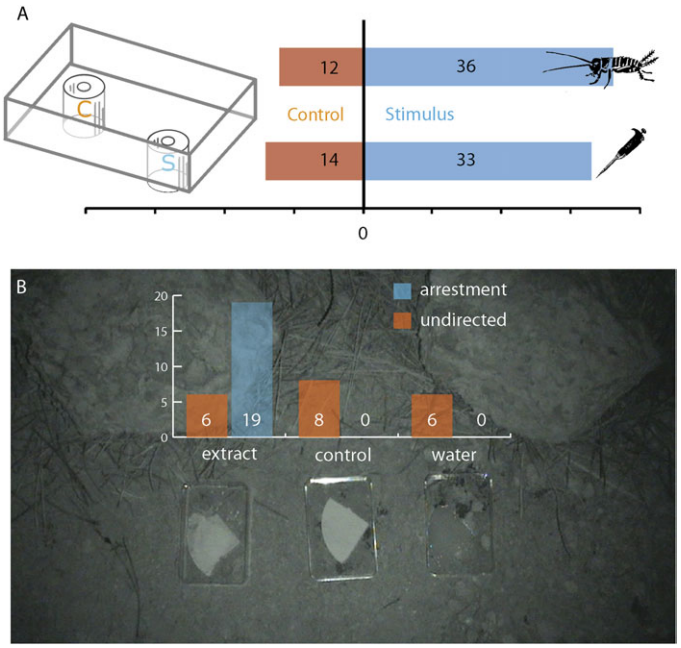

Figure 9 **(A)** Layout of the experimental arena and results of behavioral experiments with juvenile crickets and cricket extract. Single specimens were tested individually in the arena. Left-hand bars indicate the results for the control, and Right-hand bars indicate the results for the stimulus. Upper row: experiments with juveniles of *Acheta domesticus* as stimulus (n = 48 individual experiments); lower row: experiments with cricket extract as stimulus (n = 47 individual experiments). **(B)** Infrared video snapshot of the experimental layout under field conditions with 3 different filter papers in plastic dishes. Left: cricket extract (chemical stimulus), middle: control, and right: water. Video tapes covering 3 experiments that lasted 1 night were analyzed. In each experiment, 5 specimens were tested. Diagram indicates the total number of visits at the plastic dishes and the observed behavior. Left: undirected behavior at the filter paper and Right: arrestment behavior. This figure appears in color in the online version of *Chemical Senses*.

obviously many more elongated neuropils present in this region: A1, A4, A6, D4, D5 (Figure 3A,B).

In the hexapod olfactory system, axons extending from the base of the antennae undergo a sorting process such that smaller bundles are directed to their target glomeruli (Rössler et al. 1999). In malacostracan Crustacea, sensory axons from antenna 1 enter a distinct axon sorting zone, in which thinner axons projecting toward the olfactory lobe separate from thicker axons targeting the lateral antenna 1 neuropil, a mechanosensory processing unit (Schmidt and Ache 1992). Similarly, in *S. coleoptrata*, axons sort out and obtain distinctive trajectories: thinner OSNs and thicker mechanosensory axons are observable (Figure 8B). Inside the glomeruli, the afferents carry numerous boutons that indicate synaptic output. Olfactory glomeruli in honeybees have a concentric organization (Pareto 1972; Arnold et al. 1985; Fonta et al. 1993; Sun et al. 1993; Galizia et al. 1999; Nishino et al. 2005): the periphery is innervated by the axons of OSNs. Projection neurons innervate the periphery and the central core and different populations of local interneurons innervate central and peripheral areas. In those hexapods examined, ASTir neurites in the antennal lobe originate from local interneurons, projections neurons, and centrifugal neurons (reviewed in Schachtner et al. 2005). In the honeybee, ASTir neurites innervate the central core area of the glomeruli (Kreissl et al. 2010). The ASTir neurites form bleb-like boutons, and in addition few ASTir neurites branch in the peripheral glomerulus layers, making occasional synapses possible between OSNs and ASTir local interneurons. In the cockroach, ramifications extend throughout the whole glomerulus (reviewed in Schachtner et al. 2005). Schachtner et al. (2005) assumed that the possession of centrifugal ASTir neurites might be a plesiomorphic character for the Tetraconata but it is not sure from our data if similar centrifugal neurons exist in *S. coleoptrata* too. The architecture of single ONs in *S. coleoptrata* differs in shape and OSN innervation shows no specific pattern to the periphery. ASTir neurons target the whole neuropils and form buttons across its volume (Figure 6D). A longitudinal subdivision of the glomeruli into the cap, subcap, and base regions has been well documented in crayfish, clawed and clawless lobsters, and hermit crabs (Sandeman and Luff 1973; Sandeman and Sandeman 1994; Langworthy et al. 1997; Schmidt and Ache 1997; Wachowiak et al. 1997; Harzsch and Hansson 2008). In histological sections of *S. coleoptrata*, there is not any evidence of further partitions within the ONs, in contrast to layering that hallmarks columns in the olfactory lobe of malacostracan crustaceans (Sandeman et al. 1992; Harzsch and Hansson 2008).

With an average volume of approximately 443 500 μm^3, a single ON of *S. coleoptrata* is quite large in comparison to most other arthropod taxa. Single glomeruli in the olfactory lobe of the largest living land arthropod, the giant robber crab *Birgus latro* have a volume of approximately 280 000 μm^3 (Krieger et al. 2010). The olfactory glomeruli of Hexapoda are smaller and range for example between 1000 and 10 000 μm^3 in the ant *Camponotus japonicus* (Nishikawa et al. 2008) and approximately 4000 μm^3 in *D. melanogaster* (after Pinto et al. 1988). Male-specific macroglomeruli in Lepidoptera can reach a much higher volume, e.g. 300 000 μm^3 in the European corn borer *Ostrinia nubilalis* (Kárpáti et al. 2008) and 3 430 000 μm^3 in the tobacco hawkmoth *M. sexta*, in which also smaller glomeruli are present such as the club glomerulus with 187 323 μm^3 (Huetteroth and Schachter 2005).

The number of glomeruli is often considered a good estimate of the number of olfactory receptor proteins (ORs) expressed in antennal OSNs. For example, *D. melanogaster* with approximately 48 glomeruli expresses 62 functional ORs (Vosshall and Stocker 2007) and *Apis mellifera* with approximately 160–170 glomeruli expresses 170 ORs (Robertson and Wanner 2006). Most other hexapods investigated fall in between these extremes. In *S. coleoptrata*, we found 34 ONs suggesting a similar number of ORs, if the molecular basis in this species resembles that in hexapods. Ants, however, have a much higher number of glomeruli

and might thus express more than 10 times more ORs than *S. coleoptrata* does.

Can centipedes smell?

Our results clearly show that the neuronal substrate of olfaction is present in the deutocerebrum of *S. coleoptrata*. Additional support for the presumptive capability to detect airborne stimuli was obtained in the behavioral experiments. Early ethological experiments with *L. forficatus* (Lithobiomorpha) were conducted by Hennings (1904) and Friedel (1928). In their experimental setup, they presented liquids of meat to the animals, which were able to locate the stimulus or reacted with antennal tremor. Antenna amputated animals did not show any reaction. In contrast, Scharmer (1935) obtained contradictory results for *L. forficatus* with the same experimental setup. Simon (1960) described the key stimuli for *L. forficatus* as tactile or gustatory and characterized the species as a lurking predator. Finally, Meske (1961) again conducted ethological experiments on the olfactory capability of *L. forficatus*. He showed that antennal cleaning behavior was enhanced by presenting high concentrations of butanoic acid and when presenting mashed earthworms ("*Regenwurmsaft*"). Simple choice experiments carried out by Meske (1961) suggested that *L. forficatus* is able to detect the smell of meat and therefore should be able to detect an airborne stimulus. Comparable experiments with *S. coleoptrata* were only conducted by Klingel (1960). He designed an experimental arena consisting of a terrarium equipped with a perforated tube filled with living flies. In his experiments, 10 specimens of *S. coleoptrata* never noticed the presented prey during a period of 1 hour. In addition, experiments with mashed flies ("*Fliegensaft*") absorbed in a cotton ball, also failed to create any reaction. Klingel (1960) concluded that *S. coleoptrata* recognizes prey only by chemotactile stimulation.

Our own behavioral experiments contradict these results, even though we do not know if our experimental setup, the feeding conditions, and the daytime of the experiments match that of Klingel (1960). By testing starved specimens during their activity period at night and providing a longer time period to locate the prey than Klingel (1960) did, we achieved unambiguous results showing that *S. coleoptrata* is indeed able to detect airborne stimuli, both from live prey and from a chemical extract of the prey. These results are in line with the morphological findings concerning the well-developed olfactory centers in the deutocerebrum of this species.

Tactile stimuli perceived by the walking appendages have been suggested to play an important role for capturing prey in *S. coleoptrata* but it is unclear whether visual stimuli are also involved in this behavior (Meyer-Rochow et al. 2006; Rosenberg 2009). Considering that many Chilopoda including *S. coleoptrata* are active mostly during night time (Rosenberg 2009) it seems reasonable to argue that not only mechanoreceptive but also chemoreceptive abilities are the major sensory modalities involved in hunting for prey. Our video observations show that in darkness, the animals take notice of the extract and when coming into the vicinity of the extract-impregnated filter paper they immediately show the arrestment behavior suggesting that they perceive chemotactile stimuli with their antennae or walking limbs. It has been well documented that Chilopoda display a distinct cleaning behavior and especially *S. coleoptrata* spends much time in thoroughly cleaning legs and antennae (Rosenberg et al. 2004; Rosenberg 2009). Preliminary data indicate that the antennae of adult specimens are equipped with more than 2000 sensilla that can be divided into 5 different classes based on morphological criteria (Ernst A, Sombke A, Rosenberg J, in preparation). Putative chemosensory sensilla bear terminal pores. It is unclear yet if these sensilla respond to olfactory or gustatory stimuli. However, we interpret the arrestment behavior toward the cricket extract-impregnated filter papers recorded in the behavioral field experiments in total darkness as additional evidence that the animals do also react to volatile substances. The sum of both behaviors recorded on the extract was significantly higher than on the 2 controls, suggesting that an airborne stimulus can be perceived. In closer proximity, contact chemosensory perception (arrestment and probing) is suggested to be the main behavioral feature.

Mechanosensory neuropils in the deutocerebrum of Chilopoda and other Euarthropoda

In a brief description of the deutocerebral neuropils of the centipede *L. forficatus* (Lithobiomorpha), Strausfeld et al. (1995) described that the antennal nerve innervates the antennal lobe and that a lateral strand of the antennal nerve bypasses the glomeruli to project toward a region behind it, which the authors called dorsal lobe in analogy to hexapods. This posterior neuropil in the deutocerebrum was termed *masse lamelleuse* by Saint-Remy (1887) and later latinized by Fahlander (1938) who called it corpus lamellosum.

Mechanosensory neuropils with a general striate or palisade shape are also known from apterygote Hexapoda and Crustacea (reviewed in Strausfeld 1998). For instance, in the firebrat *Thermobia* sp. the neuropil innervated by their antennae is organized in a columnar and striate manner. According to our histochemical labeling against f-actin and dextran-biotin backfills, this corpus lamellosum in *S. coleoptrata* is composed of 7 to 8 parallel lamellae. In Pterygota, the first and second antennomeres supply the AMMC (Rospars 1988) whereas the flagellum is mostly specialized for olfactory perception and supplies the antennal lobe. Although we have a good understanding of the antennal olfactory pathways in hexapods, far less is known about the destination of antennal mechanosensory and gustatory receptor neurons. Unlike olfactory afferents, which project into the olfactory glomeruli, mechanosensory and gustatory

afferents project into the posterior dorsal region of the deutocerebrum and the anterior region of the subesophageal ganglion for example in *Periplaneta americana* (Burdohan and Comer 1996; Nishino et al. 2005), *A. mellifera* (Kloppenburg 1995), *Gryllus bimaculatus* (Staudacher 1998; Staudacher and Schildberger 1999), and *Aedes aegypti* (Ignell and Hansson 2005; Ignell et al. 2005). In these organisms, olfactory afferents are characterized by thin axons, whereas presumptive tactile afferents provide 2 pairs of long branches and several short branches oriented laterally and medially forming a multilayered arrangement in the dorsal lobe. Such an arrangement of short lateral and medial branches is also present in the corpus lamellosum of *S. coleoptrata*. The functional role of 2 centers (dorsal lobe and target site in the subesophageal ganglion) in hexapods could be assessed from their morphological interaction with other neuropils (Nishino et al. 2005). In the cockroach, the proximity to afferents from the maxillary palp allows the integration of signals of a similar quality detected by different peripheral organs. By the location near the antennal olfactory processing center, tactile and gustatory information may be combined with remote airborne sensory signals in the antennal lobe to obtain an integrated picture of the external world (Nishino et al. 2005).

In the present report, we also observed projections of the antennal nerve into the ventrolateral protocerebrum and the subesophageal ganglion. Fahlander (1938) was unsure whether these bundles of neurites were afferents or efferents associated with the antenna. Our data suggest that these afferents may project to gustatory centers in the subesophageal ganglion (as mentioned above in comparison to the cockroach). The projections to the ventrolateral protocerebrum may terminate close to the postantennal organ, which was described to function as a carbon dioxide receptive organ in the Japanese house centipede *Thereuonema hilgendorfi* (Yamana et al. 1986). In the mosquito *A. aegypti* (Ignell and Hansson 2005) an antenno-subesophageal tract contains axons originating from the maxillary palps and extends into the dorsal region of the antennal lobe. Whether a similar tract from the subesophageal ganglia into the antennal lobe occurs in *S. coleoptrata* is unclear.

Malacostracan crustaceans possess 2 pairs of antennae, a first, mostly chemosensory pair associated with the deutocerebrum, and a second, mostly mechanosensory pair associated with the tritocerebrum (overviews in Sandeman and Luff 1973; Blaustein et al. 1988; Sandeman et al. 1992; Schmidt and Ache 1992, 1996a; Mellon and Alones 1993; Schachtner et al. 2005). Mechanosensory and nonolfactory chemosensory input from the first antennae is processed in the lateral antennular neuropil (LAN) and the medial antennular neuropil (MAN) (Schmidt et al. 1992; Schmidt and Ache 1996a; Harzsch and Hansson 2008). Between the lobes of the lateral antenna 1 neuropil, contralateral connections occur in Decapoda. The unpaired medial antenna 1 neuropil receives input from both first antennae. Afferents from the statocysts and other mechanosensory hairs on the antennal base also project into this neuropil (Yoshino et al. 1983; Roye 1986; Schmidt and Ache 1996a). These general architectural features of the mechanosensory neuropils associated with antenna 1 in Crustacea in many respects matches the structural characteristics and connections of the corpus lamellosum in *S. coleoptrata*.

It is well known that the antenna 2 neuropils of those decapods with long second antennae often exhibit a repeated geometrical structure in which the neuropil is transversely segmented (Tautz and Müller-Tautz 1983). Sandeman DC (unpublished results) suggests that there could be a spatiotopic mapping of the antennal mechanoreceptors along the length of the antennal neuropil. Behavioral studies on the attacking behavior that can be released by lightly touching the antennae of blinded crayfish suggest that the animals know where on the antenna they have been stimulated, as they direct the chelae quite precisely to the point of contact (Sandeman in Harzsch et al. forthcoming). It remains to be explored how the architecture of this tritocerebral mechanosensory neuropil relates to that of deutocerebral mechanosensory neuropils in Hexapoda and Chilopoda.

Phylogenetic implications

The fossil record of Myriapoda spans 420 million years (Edgecombe and Giribet 2007; Shear and Edgecombe 2010). Therefore, the adaptation toward an exclusively terrestrial mode of life can be traced back to upper Silurian myriapods. Our results show that the shape of the ONs in *S. coleoptrata* is strikingly different when compared with those in hexapods and malacostracan crustaceans. These differences suggest that upon conquering land, the Myriapoda followed their own distinct pathway in evolving an olfactory system suited for aerial olfaction (compare Sombke et al. 2009). Nevertheless, in our view the presence of distinct neuropils for chemosensory and mechanosensory qualities in *S. coleoptrata*, malacostracan Crustacea, and Hexapoda could indicate a common architectural principle within the Mandibulata. Malacostracan and hexapod olfactory lobes are similar insofar as both serve the homologous pair of appendages, the antennules, equipped with OSNs (Strausfeld 2009). By analogy, a chemosensory function for the ONs and a mechanosensory function for the corpus lamellosum have been suggested (Sombke et al. 2009). In-depth comparisons of species within and across tetraconate taxa (Hexapoda and Crustacea), however, demonstrate that many characters of the organization of tetraconate olfactory centers are shared among distantly related clades but have been modified in various taxon-specific ways (Schachtner et al. 2005). Another similarity between hexapod and malacostracan olfactory systems is that in stomatopod crustaceans, which are classified as basal eumalacostracans (Abele 1991), the antennular lobes comprise discrete glomeruli, not columns. This is also true for marine isopods (Harzsch S, Hansson BS, in preparation). In contrast to

Strausfeld (1998) and Fanenbruck et al. (2004), it can be assumed that a glomerular olfactory (or antennal) lobe is a plesiomorphic character for mandibulates as proposed by Schachtner et al. (2005). This suggests that contra Harzsch (2006, 2007), the absence of olfactory lobes in, for example, the Branchiopoda and certain Maxillopoda is a reduction.

Supplementary material

Supplementary material can be found at http://www.chemse.oxfordjournals.org/.

Funding

Max Planck Society; grant DFG HA 2540/8 to Steffen Harzsch.

Acknowledgements

The authors would like to thank Carsten H.G. Müller (Greifswald) and the participants of several field trips to the Mediterranean to collect specimens of *Scutigera coleoptrata*. Verena Rieger (Greifswald) kindly conducted the western blots. We gratefully acknowledge E. Bucher (Würzburg) and H. Agricola (Jena) for generously providing samples of the Synorf 1 and Allatostatin antibodies. Our special thanks go to Nicholas J. Strausfeld (University of Arizona, USA) and to Jörg Rosenberg (Bergheim) for advice and inspiring discussions. We wish to thank Andreas Reinecke and Markus Knaden (Jena), Meike Kilian (Rostock), Stefan Fischer (Bremen), and Elisabeth Lipke (Aachen) for their help on various aspects of this project.

References

Abele LG. 1991. Comparison of morphological and molecular phylogeny of the Decapoda. Mem Queensl Mus. 31:101–108.

Anton S, Homberg U. 1999. Antennal lobe structure. In: Hansson BS, editor. Insect olfaction. Berlin (Germany): Springer. p. 97–124.

Arnold G, Masson C, Budharugsa S. 1985. Comparative study of the antennal lobes and their afferent pathway in the worker bee and the drone (*Apis mellifera*). Cell Tissue Res. 242:593–605.

Beltz BS, Kordas K, Lee MM, Long JB, Benton JL, Sandeman DC. 2003. Ecological, evolutionary, and functional correlates of sensilla number and glomerular density in the olfactory system of decapod crustaceans. J Comp Neurol. 455:260–269.

Bendena WG, Donly BC, Tobe SS. 1999. Allatostatins: a growing family of neuropeptides with structural and functional diversity. In: Sandman CA, Strand FL, Beckwith B, Chronwall BM, Flynn FW, Nachman RJ, editors. Neuropeptides: structure and function in biology and behavior. New York: Academy of Sciences. p. 311–329.

Berg BG, Galizia CG, Brandt R, Mustaparta H. 2002. Digital atlases of the antennal lobe in two species of tobacco budworm moths, the oriental *Helicoverpa assulta* (male) and the American *Heliothis virescens* (male and female). J Comp Neurol. 446:123–134.

Berg BG, Schachtner J, Homberg U. 2009. γ-Aminobutyric acid immunostaining in the antennal lobe of the moth *Heliothis virescens* and its colocalization with neuropeptides. Cell Tissue Res. 335: 593–605.

Berg BG, Schachtner J, Utz S, Homberg U. 2007. Distribution of neuropeptides in the primary olfactory center of the heliothine moth *Heliothis virescens*. Cell Tissue Res. 327:385–398.

Blaustein DN, Derby CD, Simmons RB, Beall AC. 1988. Structure of the brain and medulla terminals of the spiny lobster *Panulirus argus* and the crayfish *Procambarus clarkii* with an emphasis on olfactory centers. J Crustacean Biol. 8:493–519.

Burdohan JA, Comer CM. 1996. Cellular organization of an antennal mechanosensory pathway in the cockroach *Periplaneta americana*. J Neurosci. 16:5830–5843.

Burggren WW, McMahon BR. 1988. Biology of the land crabs. New York: Cambridge University Press. p. 492.

Cebia F. 2008. Organization of the nervous system in the model planarian *Schmidtea mediterranea*: an immunocytochemical study. J Neurosci Res. 61:375–384.

Chambille I, Rospars JP. 1981. Le deutocerebron de la blatte *Blaberus craniifer* Burm. (Dictyoptera: Blaberidae). Étude qualitative et identification visuelle des glomerules. Int J Insect Morphol Embryol. 10: 141–165.

Cook CE, Smith ML, Telford MJ, Bastianello A, Akam M. 2001. Hox genes and the phylogeny of the arthropods. Curr Biol. 11:759–763.

Dockray GJ. 2004. The expanding family of -RFamide peptides and their effects on feeding behaviour. Exp Physiol. 89:229–235.

Dohle W. 2001. Are the insects terrestrial crustaceans? A discussion of some new facts and arguments and the proposal of the proper name "Tetraconata" for the monophyletic unit Crustacea + Hexapoda. Ann Soc Entomol Fr. 37:85–103.

Dreyer D, Vitt H, Dippel S, Goetz B, el Jundi B, Kollmann M, Huetteroth W, Schachtner J. 2010. 3D standard brain of the red flour beetle *Tribolium castaneum*: a tool to study metamorphic development and adult plasticity. Front Syst Neurosci. 4:3.

Edgecombe GD, Giribet G. 2007. Evolutionary biology of centipedes (Myriapoda: Chilopoda). Annu Rev Entomol. 52:151–170.

Eisthen HL. 2002. Why are olfactory systems of different animals so similar? Brain Behav Evol. 59:273–293.

Fahlander K. 1938. Beiträge zur Anatomie und systematischen Einteilung der Chilopoden. Zool Bidrag Uppsala. 17:1–148.

Fanenbruck M, Harzsch S, Wägele JW. 2004. The brain of the Remipedia (Crustacea) and an alternative hypothesis on their phylogenetic relationships. Proc Natl Acad Sci U.S.A. 101:3868–3873.

Fonta C, Sun X-J, Masson C. 1993. Morphology and spatial distribution of bee antennal lobe interneurons responsive to odours. Chem Senses. 18:101–119.

Friedel H. 1928. Ökologische und physiologische Untersuchungen an *Scutigerella immaculata*. Z Morphol Ökol Tiere. 10:738–797.

Galizia CG, McIlwrath SL, Menzel R. 1999. A digital three-dimensional atlas of the honey-bee antennal lobe based on optical sections acquired by confocal microscopy. Cell Tissue Res. 395:383–394.

Galizia CG, Menzel R. 2000. Odour perception in honeybees: coding information in glomerular patterns. Curr Opin Neurobiol. 10:504–510.

Galizia CG, Menzel R. 2001. The role of glomeruli in the neural representation of odours: results from optical recording studies. J Insect Physiol. 47:115–130.

Ghaninia M, Hansson BS, Ignell R. 2007. The antennal lobe of the African malaria mosquito, *Anopheles gambiae*—innervations and three dimensional reconstruction. Arthropod Struct Dev. 36:23–39.

Greenberg MJ, Price DA. 1992. Relationships among the FMRFamidelike peptides. Prog Brain Res. 92:25–37.

Hansson BS, Christensen TA. 1999. Functional characteristics of the antennal lobe. In: Hansson BS, editor. Insect olfaction. Berlin (Germany): Springer. p. 125–161.

Harzsch S. 2006. Neurophylogeny: architecture of the nervous system and a fresh view on arthropod phylogeny. Int Comp Biol. 46:162–194.

Harzsch S. 2007. The architecture of the nervous system provides important characters for phylogenetic reconstructions: examples from the Arthropoda. Species Phylogeny Evol. 1:33–57.

Harzsch S, Hansson BS. 2008. Brain architecture in the terrestrial hermit crab *Coenobita clypeatus* (Anomura, Coenobitidae): neuroanatomical evidence for a superb aerial sense of smell. BMC Neurosci. 9:1–35.

Harzsch S, Melzer RR, Müller CHG. 2007. Mechanisms of eye development and evolution of the arthropod visual system: the lateral eyes of myriapoda are not modified insect ommatidia. Org Divers Evol. 7:20–32.

Harzsch S, Müller CHG. 2007. A new look at the ventral nerve centre of *Sagitta*: implications for the phylogenetic position of Chaetognatha (arrow worms) and the evolution of the bilaterian nervous system. Front Zool. 4:14.

Harzsch S, Sandeman D, Chaigneau J. Forthcoming. Morphology and development of the central nervous system. In: Forest J, von Vaupel Klein JC, editors. Treatise on zoology—Crustacea. Vol. 3. Leiden (The Netherlands): Koninklijke Brill Academic Publishers.

Hennings C. 1904. Zur Biologie der Myriapoden II. Geruch und Geruchsorgane der Myriapoden. Biol Zent Bl. 16:251–274–256282.

Homberg U. 1994. Distribution of neurotransmitters in the insect brain. Prog Zool. 40:1–88.

Homberg U. 2005. Multisensory processing in the insect brain. In: Christensen TA, editor. Methods in insect sensory neuroscience. Boca Raton (FL): CRC Press. p. 3–25.

Hörberg T. 1931. Studien über den komparativen Bau des Gehirns von *Scutigera coleoptrata* L. 2 Lunds Universitets Årsskrift N.F. Avd. 27:1–24.

Huetteroth W, Schachter J. 2005. Standard three-dimensional glomeruli of the *Manduca sexta* antennal lobe: a tool to study both developmental and adult neuronal plasticity. Cell Tissue Res. 319:513–524.

Hwang UW, Friedrich M, Tautz D, Park CJ, Kim W. 2001. Mitochondrial protein phylogeny joins myriapods with chelicerates. Nature. 413:154–157.

Ignell R, Dekker T, Ghaninia M, Hansson BS. 2005. Neuronal architecture of the mosquito deutocerebrum. J Comp Neurol. 493:207–240.

Ignell R, Hansson BS. 2005. Projection patterns of gustatory neurons in the suboesophageal ganglion and tritocerebrum of mosquitoes. J Comp Neurol. 492:214–233.

Kárpáti Z, Dekker T, Hansson BS. 2008. Reversed functional topology in the antennal lobe of the male European corn borer. J Exp Biol. 211: 2841–2848.

Kirschner S, Kleineidam CJ, Zube C, Rybak J, Grünewald B, Rössler W. 2006. Dual olfactory pathway in the honeybee, *Apis mellifera*. J Comp Neurol. 499:933–952.

Klagges BRE, Heimbeck G, Godenschwege TA, Hofbauer A, Pflugfelder GO, Reifegerste R, Reisch D, Schaupp M, Buchner S, Buchner E. 1996. Invertebrate synapsins: a single gene codes for several isoforms in Drosophila. J Neurosci. 16:3154–3165.

Klingel H. 1960. Vergleichende Verhaltensbiologie der Chilopoden *Scutigera coleoptrata* L. ("Spinnenassel") und *Scolopendra cingulata* Latreille (Skolopender). Z Tierpsychol. 17:11–30.

Kloppenburg P. 1995. Anatomy of the antennal motor neurons in the brain of the honeybee (*Apis mellifera*). J Comp Neurol. 363:333–343.

Kreis TE. 1987. Microtubules containing detyrosinated tubulin are less dynamic. EMBO J. 6:2597–2606.

Kreissl S, Strasser C, Galizia CG. 2010. Allatostatin immunoreactivity in the honeybee brain. J Comp Neurol. 518:1391–1417.

Krieger J, Sandeman RE, Sandeman DC, Hansson BS, Harzsch S. 2010. Brain architecture of the largest living land arthropod, the Giant Robber Crab *Birgus latro* (Crustacea, Anomura, Coenobitidae): evidence for a prominent central olfactory pathway? Frontiers in Zoology. 7:25.

Laissure PP, Reiter C, Hiesinger PR, Halter S, Fischbach KF, Stocker RF. 1999. Three-dimensional reconstruction of the antennal lobe in *Drosophila melanogaster*. J Comp Neurol. 405:543–552.

Langworthy K, Helluy S, Benton J, Beltz B. 1997. Amines and peptides in the brain of the American lobster: immunocytochemical localization patterns and implications for brain function. Cell Tissue Res. 288:191–206.

Loesel R, Nässel DR, Strausfeld NJ. 2002. Common design in a unique midline neuropil in the brains of arthropods. Arthropod Struct Dev. 31: 77–91.

Mallatt JM, Garey JR, Shultz JW. 2004. Ecdysozoan phylogeny and Bayesian inference: first use of nearly complete 28S and 18S rRNA gene sequences to classify the arthropods and their kin. Mol Phylogenet Evol. 31:178–191.

Mellon D, Alones V. 1993. Cellular organization and growth-related plasticity of the crayfish olfactory midbrain. Microsc Res Tech. 24: 231–259.

Melzer RR, Petyko Z, Smola U. 1996. Photoreceptor axons and optic neuropils in *Lithobius forficatus* (Linnaeus, 1758) (Chilopoda, Lithobiidae). Zool. Anz. 235:177–182.

Meske C. 1961. Untersuchungen zur Sinnesphysiologie von Diplopoden und Chilopoden. Z Vgl Physiol. 45:61–77.

Meyer-Rochow VB, Müller CHG, Lindström M. 2006. Spectral sensitivity of the eye of *Scutigera coleoptrata* (Linnaeus, 1758) (Chilopoda: Scutigeromorpha: Scutigeridae). Appl Entomol Zool. 41:117–122.

Müller CHG, Sombke A, Rosenberg J. 2007. The fine structure of the eyes of some bristly millipedes (Penicillata, Diplopoda): additional support for the homology of mandibulate ommatidia. Arthropod Struct Dev. 36:463–476.

Nässel DR. 1993. Neuropeptides in the insect brain: a review. Cell Tissue Res. 273:1–29.

Nässel DR, Homberg U. 2006. Neuropeptides in interneurons of the insect brain. Cell Tissue Res. 326:1–24.

Negrisolo E, Minelli A, Valle G. 2004. The mitochondrial genome of the house centipede *Scutigera* and the monophyly versus paraphyly of myriapods. Mol Biol Evol. 21:770–780.

Nishikawa M, Nishino H, Misaka Y, Kubota M, Tsuji E, Satoji Y, Ozaki M, Yokohari F. 2008. Sexual dimorphism in the antennal lobe of the ant *Camponotus japonicus*. Zool Sci. 25:195–204.

Nishino H, Nishikawa M, Yokohari F, Mizunami M. 2005. Dual, multilayered somatosensory maps formed by antennal tactile and contact chemosensory afferents in an insect brain. J Comp. Neurol. 493:291–308.

Pareto A. 1972. Die zentrale Verteilung der Fühlerafferenz bei Arbeiterinnen der Honigbiene, *Apis mellifera*, L. Z Zellforsch Mikrosk Anat. 131: 109–140.

Pinto L, Stocker RF, Rodriguesa V. 1988. Anatomical and neurochemical classification of the antennal glomeruli in *Drosophila melanogaster*

Meigen (Diptera: Drosophilidae). Int J Insect Morphol Embryol. 17: 335–344.

Pisani D, Poling LL, Lyons-Weiler M, Hedges SB. 2004. The colonization of land by animals: molecular phylogeny and divergence times among arthropods. BMC Biol. 2:1–10.

Popadic A, Panganiban G, Rusch D, Shear WA, Kaufman TC. 1998. Molecular evidence for the gnathobasic derivation of arthropod mandibles and for the appendicular origin of the labrum and other structures. Dev Genes Evol. 208:142–150.

Powers LW, Bliss DE. 1983. Terrestrial adaptations. In: Verneberg FJ, Vernberg WB, editors. The biology of Crustacea, Vol. 8: environmental adaptations. New York: Academic Press. p. 272–333.

Price DA, Greenberg MJ. 1989. The hunting of the FaRPs: the distribution of FMRFamide-related peptides. Biol Bull. 177:198–205.

Regier JC, Shultz JW, Zwick A, Hussey A, Ball B, Wetzer R, Martin JW, Cunningham CW. 2010. Arthropod relationships revealed by phylogenomic analysis of nuclear protein-coding sequences. Nature. 463:1079–1083.

Richter S. 2002. The Tetraconata concept: hexapod–crustacean relationships and the phylogeny of Crustacea. Org Divers Evol. 2:217–237.

Rieger V, Perez Y, Müller CHG, Lipke E, Sombke A, Hansson BS, Harzsch S. 2010. Immunohistochemical analysis and 3D reconstruction of the cephalic nervous system in Chaetognatha: insights into the evolution of an early bilaterian brain? Invertebr Biol. 129:1–26.

Robertson HM, Wanner KW. 2006. The chemoreceptor superfamily in the honey bee, *Apis mellifera*: expansion of the odorant, but not gustatory, receptor family. Genome Res. 16:1395–1403.

Rosenberg J. 2009. Die Hundertfüßer: Chilopoda. Die Neue Brehm-Bücherei Bd. 285. Hohenwarsleben (Germany): Westarp Wissenschaften. p. 524.

Rosenberg J, Brenner M, Greven H. 2004. Putzverhalten und Trinken bei *Scutigera coleoptrata* L. (Chilopoda, Scutigeromorpha). Entomol Heute. 16:83–92.

Rospars JP. 1983. Invariance and sex-specific variations of the glomerular organization in the antennal lobes of a moth, *Mamestra brassicae* and a butterfly, *Pieris brassicae*. J Comp Neurol. 220:80–96.

Rospars JP. 1988. Structure and development of the insect antennodeutocerebral system. Int J Insect Morphol Embryol. 17:243–294.

Rospars JP, Hildebrand JG. 1992. Anatomical identification of glomeruli in the antennal lobes of the male sphinx moth *Manduca sexta*. Cell Tissue Res. 270:205–227.

Rössler W, Oland LA, Higgins MR, Hildebrandt JG, Tolbert LP. 1999. Development of a glia-rich axon-sorting zone in the olfactory pathway of the moth *Manduca sexta*. The Journal of Neuroscience. 19(22):9865–9877.

Roye DB. 1986. The central distribution of movement sensitive afferent fibers from the antennular short hair sensilla of *Calinectes sapidus*. Mar Freshw Behav Physiol. 12:181–196.

Saint-Remy G. 1887. Contribution a l'étude du cerveau chez les arthropods trachéates. Arch Zool Exp Gen. 2:1–274.

Saint-Remy G. 1889. Sur la structure du cerveau chez les Myriapodes et les Arachnides. Rev Biol Nord France. 8:281–298.

Sandeman DC, Luff SE. 1973. The structural organization of glomerular neuropile in the olfactory and accessory lobes of an australian freshwater crayfish, *Cherax destructor*. Z Zellforsch Mikrosk Anat. 142:37–61.

Sandeman DC, Sandeman RE. 1994. Electrical responses and synaptic connections of giant serotonin-immunoreactive neurons in crayfish olfactory and accessory lobes. J Comp Neurol. 341:130–144.

Sandeman DC, Sandeman RE, Derby C, Schmidt M. 1992. Morphology of the brain of crayfish, crabs, and spiny lobsters: a common nomenclature for homologous structures. Biol Bull. 183:304–326.

Sandeman DC, Scholtz G, Sandeman RE. 1993. Brain evolution in decapods Crustacea. J Exp Zool. 65:112–133.

Schachtner J, Schmidt M, Homberg U. 2005. Organization and evolutionary trends of primary olfactory brain centers in Tetraconata (Crustacea+ Hexapoda). Arthropod Struct Dev. 34:257–299.

Scharmer J. 1935. Die Bedeutung der Rechts-Links-Struktur und die Orientierung bei *Lithobius forficatus*. Zool Jahrb Abt Allg Zool Physiol. 54:459–506.

Schmidt M, Ache BW. 1992. Antennular projections to the midbrain of the spiny lobster. II. Sensory innervation of the olfactory lobe. J Comp Neurol. 318:291–303.

Schmidt M, Ache BW. 1996a. Processing of antennular input in the brain of the spiny lobster, *Panulirus argus*. I. Non-olfactory chemosensory and mechanosensory pathway of the lateral and median antennular neuropils. J Comp Physiol A. 178:579–604.

Schmidt M, Ache BW. 1996b. Processing of antennular input in the brain of the spiny lobster, *Panulirus argus*. II. The olfactory pathway. J Comp Physiol A. 178:605–628.

Schmidt M, Ache BW. 1997. Immunocytochemical analysis of glomerular regionalization and neuronal diversity in the olfactory deutocerebrum of the spiny lobster. Cell and Tissue Research. 287:541–563.

Schmidt M, van Ekeris L, Ache BW. 1992. Antennular projections to the midbrain of the spiny lobster. I. Sensory innervation of the lateral and medial antennular neuropils. J Comp Neurol. 318:277–290.

Seifert G. 1967. Das stomatogastrische Nervensystem der Chilopoden. Zool Jahrb Abt Anat Ontogenie Tiere. 84:167–190.

Shear WA, Edgecombe G. 2010. The geological record and phylogeny of the Myriapoda. Arthropod Struct Dev. 39:174–190.

Simon H-J. 1960. Zur Ernährungsbiologie von *Lithobius forficatus*. Zool Anz. 164:19–26.

Sombke A, Harzsch S, Hansson BS. 2009. Brain structure of *Scutigera coleoptrata*: new insights into the evolution of mandibulate olfactory centers—short communication. Soil Org. 81:319–325.

Staudacher E. 1998. Distribution and morphology of descending brain neurons in the cricket. Cell Tissue Res. 294:187–202.

Staudacher E, Schildberger K. 1999. A newly described neuropile in the deutocerebrum of the cricket: antennal afferents and descending interneurons. Zoology. 102:212–226.

Strausfeld NJ. 1980. The Golgi method: its application to the insect nervous system and the phenomenon of stochastic impregnation. In: Strausfeld NJ, Miller TA, editors. Neuroanatomical techniques. Insect nervous system. New York: Springer. p. 132–205.

Strausfeld NJ. 1998. Crustacean–insect relationships: the use of brain characters to derive phylogeny amongst segmented invertebrates. Brain Behav Evol. 52:186–206.

Strausfeld NJ. 2005. The evolution of crustacean and insect optic lobes and the origin of chiasmata. Arthropod Struct Dev. 34:235–256.

Strausfeld NJ. 2009. Brain organization and the origin of insects: an assessment. Proc R Soc Lond B Biol Sci. 276:1929–1937.

Strausfeld NJ, Buschbeck E, Gomez RS. 1995. The arthropod mushroom body: its functional roles, evolutionary enigmas and mistaken identities. In: Breidbach O, Kutsch W, editors. The nervous system of invertebrates an evolutionary and comparative approach. Basel (Switzerland): Birghäusler Verlag. p. 349–382.

Strausfeld NJ, Hildebrand JG. 1999. Olfactory systems: common design, uncommon origins? Curr Opin Neurobiol. 9:634–639.

Sullivan JM, Benton JL, Sandeman DC, Beltz BS. 2007. Adult neurogenesis: a common strategy across diverse species. J Comp Neurol. 500: 574–584.

Sun X-J, Fonta C, Masson C. 1993. Odour quality processing by the antennal lobe interneurons. Chem Senses. 18:355–377.

Tautz J, Müller-Tautz R. 1983. Antennal neuropile in the brain of the crayfish: morphology of neurons. J Comp Neurol. 218:415–425.

Vilpoux K, Sandeman R, Harzsch S. 2006. Early embryonic development of the central nervous system in the Australian crayfish and the Marbled crayfish (Marmorkrebs). Dev Genes Evol. 216:209–223.

Vitzthum H, Homberg U, Agricola H. 1996. Distribution of Dip-allatostatin I-like immunoreactivity in the brain of the Locust *Schistocerca gregaria* with detailed analysis of immunostaining in the central complex. J Comp Neurol. 369:419–437.

von Reumont BM, Meusemann K, Szucsich NU, Dell'Ampio E, Gowri-Shankar V, Bartel D, Simon S, Letsch HO, Stocsits RR, Luan Y, Wägele JW, et al. 2009. Can comprehensive background knowledge be incorporated into substitution models to improve phylogenetic analyses? A case study on major arthropod relationships. BMC Evol Biol. 9:119.

Vosshall LB, Stocker RF. 2007. Molecular architecture of smell and taste in Drosophila. Annu Rev Neurosci. 30:505–533.

Wachowiak M, Diebel CE, Ache BW. 1997. Local interneurons define functionally distinct regions within olfactory glomeruli. J Exp Biol. 200:989–1001.

Yamana K, Toh Y, Tateda H. 1986. Electrophysiological studies on the temporal organ of the Japanese house centipede, *Thereuonema hilgendorfi*. J Exp Biol. 126:297–314.

Yoshino M, Kondoh Y, Hisada M. 1983. Projection of statocyst sensory neurons associated with crescent hairs in the crayfish *Procambarus clarkii* Girard. Cell Tissue Res. 230:37–48.

Zajac J-M, Mollereau C. 2006. Introduction: RFamide peptides. Peptides. 27:941–942.

Zube C, Kleineidam CJ, Kirschner S, Neef J, Rössler W. 2008. Organization of the olfactory pathway and odor processing in the antennal lobe of the ant *Camponotus floridanus*. J Comp Neurol. 506:425–441.